Bio-mineral Interactions and the Environment

Giovanni De Giudici, Daniela Medas, and Carlo Meneghini

1 Biominerals: A Continuously Growing Family

Biominerals are the product of organism's activity leading to mineral formation within the cellular space or in the space surrounding the organism. In the last decades biominerals have received growing interest from a large interdisciplinary scientific community. Actually, biominerals are known from the geological record to play a pivotal role in biogeochemical cycles of elements [1, 2]. Thus, understanding biomineralization processes in widely different environments helps us to understand environmental changes induced by anthropic activities, as well the as environment resiliency [3, 4]. Moreover, they offer diverse examples to devise useful biobased materials and allow the development of technologies for environmental sustainability [5, 6]. This work is aimed to summarize our understanding of biominerals, their classification, and their impact in our society. Recent investigations on bio-mineral interactions are presented focusing on processes, investigation techniques, impact on the environment and sustainable technologies. We do not attempt to provide a comprehensive overlook of the whole field, but we place emphasis on specific aspects where we have first-hand experience.

Based on the causative effect of cellular activity, biominerals were classified for the first time by Lowenstam [7] into two main classes, namely biologically controlled mineralization (BCM) and biologically induced mineralization (BIM). More recently, Skinner [8] provided a thorough definition "*The simple definition of biominerals is that they are a subset of the mineral kingdom, created through the actions and activity of a life form. The term as used herein is meant to be very*

G. De Giudici (✉) · D. Medas
Department of Chemical and Geological Sciences, University of Cagliari, Cagliari, Italy
e-mail: gbgiudic@unica.it

C. Meneghini
Department of Sciences, University Roma Tre, Rome, Italy
e-mail: carlo.meneghini@uniroma3.it

M. Tribaudino et al. (eds.), *Minerals and Waste*, Earth and Environmental Sciences Library, https://doi.org/10.1007/978-3-031-16135-3_4

general, and inclusive of the entire range of living creatures and their products. The range extends from the primitive, not-so-well-classified forms at the very bottom of the tree of life, the Archaea, and bacteria, through the eukaryotes with well-defined morphology that may contain mineral materials in sub-cellular, or extracellular, compartments, or tissues, up to and including, vertebrates and plants".

Biominerals can be classified using the same framework as that for other minerals, by composition based on the anionic constituents, and there are representatives in almost all the 10 mineral classes listed by Strunz [9]. The already long list provided by Skinner [8] is still growing with hundreds of investigations on novel natural ecological niches around the world, or at sites created by human activities through industry and manufacturing. Interestingly, biominerals also include minerals that in geological processes form only at high temperature and pressure.

The knowledge of the diversity of biomineral composition is increasing beyond all expectations. In 1963, Lowenstam identified 10 different mineral types; this increased to 19 biominerals by 1974 [10], 30 by 1981 [7], 39 by 1983 [11], 56 by 2003 [12], and 96 by 2008 [13]. Table 1 shows a state-of-the-art list of 160 different biogenic minerals identified to date and distributed between the life kingdoms. Figure 1 shows the distribution of the 160 biominerals among the classes.

As previously mentioned, most biominerals, despite their peculiar characteristics and the intimate association of their structures with organic molecules, can be classified as common mineral species based on the anionic constituents [8]. Biomineral composition depends on both the control played by the specific (micro)organism and by the available chemical species in the environment. Then, factors such as pH, pO_2, Eh, etc. can play a significant role on the final product. This leads to substantial differences, for example, between the locations where carbonate biominerals might form and the locations where sulphides might be produced [8]. For instance, carbonate (e.g., calcite, hydrozincite) bioprecipitation can occur in neutral or slightly alkaline environments often driven by the photosynthetic activity of bacteria [14], whereas sulphides (e.g., pyrite or sphalerite) will form under the mediation of sulphur-reducing bacteria, in a reducing environment where metals are available [15]. Table 1 shows that the most commonly occurring cations in biominerals are Ca, Fe, Mg, Na and K. Calcium and Mg are mainly hosted in carbonates and phosphates, whereas Fe occurs in sulphides and oxides/hydroxides. Also, potentially harmful elements such as Cu, Mn, Zn, As, Pb, etc. can occur in biominerals belonging to several mineral classes.

2 Mineral Surfaces and Biological Interfaces

Bio-mineral interfaces are the place where different microscopic processes take place resulting in controlled or induced biomineralization. Bio-mineral interfaces are then the key to understand biomineralization processes and to develop sustainable technologies for industry and environment. These processes are intrinsically

Table 1 List of minerals produced by biological precipitation over Strunz classes. Expanded from [12, 13]

Name	Formula
Elements (01)	
α-sulfur	S
γ-sulfur (Rosickýite)	S
Sulphides (02)	
Acanthite	Ag_2S
Amorphous pyrrhotite	$Fe_{1-x}S$ (x = 0–0.17)
Galena	PbS
Greigite	Fe_3S_4
Hydrotroilite	$FeS{\cdot}nH_2O$
Löllingite [16]	$FeAs_2$
Mackinawite	$(Fe, Ni)_9S_8$
Marcasite	FeS_2
Microcrystalline millerite [17]	NiS
Pyrite	FeS_2
Pyrrhotite	Fe_7S_8
Orpiment	As_2S_3
Sphalerite	ZnS
Wurtzite	ZnS
Halides (03)	
Atacamite	$Cu_2Cl(OH)_3$
Halite	NaCl

(continued)

Table 1 (continued)

Name	Formula
Sylvite	KCl
Ammineite [18]	$CuCl_2{\cdot}2NH_3$
Amorphous fluorite [19]	CaF_2
Fluorite	CaF_2
Hieratite	K_2SiF_6
Oxides and Hydroxides (04)	
Amorphous iron titanate	$Fe^{2+}TiO_3$
Amorphous iron oxide	Fe_2O_3
Amorphous manganese oxide	Mn_3O_4
Anatase	TiO_2
Desert Varnish	MnO and FeO
Ilmenite	$FeTiO_3$
Lime [18]	CaO
Maghemite	$Fe_{2.67}O_4$
Magnetite	Fe_3O_4
Periclase	MgO
Portlandite [18]	$Ca(OH)_2$
Ice	H_2O
Amorphous mixed As(III)/As(V)-Fe(III) oxy-hydroxides [20]	
Birnessite	$NaMn_4O_8{\cdot}3H_2O$
Brucite	$Mg(OH)_2$

(continued)

Table 1 (continued)

Name	Formula
Ferrihydrite	$Fe_{4–5}(OH,O)_{12}$
Goethite	α-FeO(OH)
Lepidocrocite	γ-FeO(OH)
Todorokite	$(Na,Ca,K,Ba,Sr)_{1-x}(Mn,Mg,Al)_6O_{12}·3\text{-}4H_2O$
Tooeleite [20]	$Fe_6(AsO_3)_4(SO_4)(OH)_4.4H_2O$
Carbonates and Nitrates (05)	
Amorphous calcium carbonates	$CaCO_3·H_2O$ or $CaCO_3$
	(at least 5 forms)
Aragonite	$CaCO_3$
Baylissite [18]	$K_2Mg(CO_3)_2·4H_2O$
Bütschliite [18]	$K_2Ca(CO_3)_2$
Calcite	$CaCO_3$
Chukanovite [18]	$Fe_2(CO_3)(OH)_2$
Dypingite [21]	$Mg_5(CO_3)_4(OH)_2·5H_2O$
Fairchildite [18]	$K_2Ca(CO_3)_2$
Hydrocerussite	$Pb_3(CO_3)_2(OH)_2$
Hydrozincite [14]	$Zn_5(CO_3)_2(OH)_6$
Kalicinite [18]	$KH(CO_3)$
Lansfordite	$MgCO_3·5H_2O$
Magnesite	$MgCO_3$
Mg-calcite	$(Mg_xCa_{1–x})CO_3$

(continued)

Table 1 (continued)

Name	Formula
Monohydrocalcite	$CaCO_3 \cdot H_2O$
Nesquehonite	$Mg(CO_3) \cdot 3H_2O$
Protodolomite	$CaMg(CO_3)_2$
Rhodochrosite	$MnCO_3$
Siderite	$FeCO_3$
Strontianite [22]	$SrCO_3$
Teschemacherite [18]	$(NH_4)H(CO_3)$
Trona [18]	$Na_3(HCO_3)(CO_3) \cdot 2H_2O$
Vaterite	$CaCO_3$
Gwihabaite	$(NH_4)NO_3$
Shilovite [18]	$Cu(NH_3)_4(NO_3)_2$
Sulphates (07)	
Aphthitalite	$K_3Na(SO_4)_2$
Arcanite [18]	K^2SO^4
Ardealite	$Ca_2[PO_3(OH)](SO_4) \cdot 4H_2O$
Barite	$BaSO_4$
Bassanite [23]	$CaSO_4 \cdot 0.5H_2O$
Celestine	$SrSO_4$
Epsomite	$MgSO_4 \cdot 7H_2O$
Feynmanite [18]	$Na(UO_2)(SO_4)(OH) \cdot 3.5H_2O$
Green rust [24, 25]	$[Fe^{2+}_{(6-x)}Fe^{3+}_{(x)}(OH)_{12}]^{x+}[(A^{2-})_{x/2}.yH_2O]^{x-}$

(continued)

Table 1 (continued)

Name	Formula
Gypsum	$CaSO_4{\cdot}2H_2O$
Hexahydrite	$MgSO_4{\cdot}6H_2O$
Jarosite	$KFe^{3+}{}_3(SO^4)_2(OH)_6$
Langbeinite [18]	$K_2Mg_2(SO_4)_3$
Lecontite [18]	$(NH_4)Na(SO_4){\cdot}2H_2O$
Melanterite	$Fe^{2+}SO_4{\cdot}7H_2O$
Möhnite [18]	$(NH_4)K_2Na(SO_4)_2$
Schwertmannite	$Fe^{3+}{}_{16}O_{16}(OH)_{9.6}(SO_4)_{3.2}{\cdot}10H_2O$
Witzkeite [18]	$Na_4K_4Ca(NO_3)_2(SO_4)_4{\cdot}2H_2O$
Phosphates (08)	
Amorphous calcium phosphate (at least 6 forms)	Variable
Amorphous calcium pyrophosphate	$Ca_2P_2O{\cdot}2H_2O$
Amorphous hydrous Fe(III) phosphate	Variable
Bakhchisaraitsevite	$Na_2Mg_5(PO_4)_4{\cdot}7H_2O$
Bobierrite [18]	$Mg_3(PO_4)_2{\cdot}8H_2O$
Brushite	$Ca[PO_3(OH)]{\cdot}2H_2O$
Carbonate-hydroxylapatite (dahllite)	$Ca_5(PO_4{,}CO_3)_3(OH)$
Chlorapatite	$Ca_5(PO_4)_3Cl$
Dittmarite [18]	$(NH_4)Mg(PO_4)\cdot H_2O$
Fluorapatite	$Ca_5(PO_4)_3F$
Francolite	$Ca_{10}(PO_4)_6F_2$

(continued)

Table 1 (continued)

Name	Formula
Hannayite	$Mg_3(NH_4)_2H_4(PO_4)_4{\cdot}8H_2O$
Hopeite [18]	$Zn_3(PO_4)_2{\cdot}4H_2O$
Hazenite	$KNaMg_2(PO_4)_2{\cdot}14H_2O$
Hydroxylapatite	$Ca_5(PO_4)_3(OH)$
Monetite	$Ca[PO_3(OH)]$
Newberyite	$Mg[PO_3(OH)]{\cdot}3H_2O$
Octacalcium phosphate	$Ca_8H_2(PO_4)_6$
Pyromorphite [26]	$Pb_5[PO_4]_3(Cl, OH)$
Redondite [18]	$Al(PO_4){\cdot}2H_2O$
Schertelite [18]	$(NH_4)_2MgH_2(PO_4)_2{\cdot}4H_2O$
Stercorite [18]	$(NH_4)Na(PO_3OH){\cdot}4H_2O$
Strengite [27, 28]	$FePO_4{\cdot}2H_2O$
Struvite	$Mg(NH_4)(PO_4){\cdot}6H_2O$
Struvite-(K) [18]	$KMg(PO_4){\cdot}6H_2O$
Swaknoite [18]	$(NH_4)_2Ca(PO_3OH)_2{\cdot}H_2O$
Variscite [29]	$AlPO_4{\cdot}2H_2O$
Vivianite	$Fe_3^{2+}(PO_4)_2{\cdot}8H_2O$
Whitlockite	$Ca_{18}H_2(Mg,Fe)_2(PO_4)_{14}$
Silicates (09)	
Amorphous silica	$SiO_2{\cdot}nH_2O$
Amorphous hemimorphite [30, 31]	$Zn_4(Si_2O_7)(OH)_2{\cdot}H_2O$

(continued)

Table 1 (continued)

Name	Formula
Buddingtonite	$(NH_4)(AlSi_3O_8)$
Chamosite [17]	$(Fe_5Al)(Si_3Al)O_{10}(OH)_8$
Forsterite [32]	Mg_2SiO_4
Kaolinite [33]	$Al_4(Si_4O_{10})(OH)_4$
Kerolite [34]	$Mg_3Si_4O_{10}(OH)_2 \cdot nH_2O$
Low-ordered (Fe,Al) silicate [35]	Variable composition
Nontronite [36]	$Na_{0.3}Fe^{3+}{}_2(Si,Al)_4O_{10}(OH)_2 \cdot nH_2O$
Quartz [18]	SiO_2
Stevensite [37]	$(Ca_{0.09}K_{0.01}Sr_{0.01})_{\Sigma=0.11}(Mg_{2.84}Fe_{0.02}Al_{0.03})_{\Sigma=2.89}(Si_{3.98}Al_{0.02}O_{10})(OH)_2 \cdot nH_2O$
Organic compounds (10)	
Abelsonite	$Ni^{2+}C_{31}H_{32}N_4$
Antipinite [18]	$KNa_3Cu_2(C_2O_4)_4$
Branchite [18]	$C_{20}H_{34}$
Calclacite [18]	$Ca(CH_3COO)Cl \cdot 5H_2O$
Ca malate	$C_4H_4CaO_5$
Ca tartrate	$C_4H_4CaO_6$
Carpathite	$C_{24}H_{12}$
Chanabayaite [18]	$CuCl(N_3C_2H_2)(NH_3) \cdot 0.25H_2O$
Coskrenite-(Ce) [18]	$(Ce,Nd,La)_2(C_2O_4)(SO_4)_2 \cdot 12H_2O$
Earlandite	$Ca_3(C_6H_5O_7)_2 \cdot 4H2O$
Ernstburkeite [18]	$Mg(CH_3SO_3)_2 \cdot 12H_2O$

(continued)

Table 1 (continued)

Name	Formula
Falottaite [18]	$MnC_2O_4{\cdot}3H_2O$
Flagstaffite [18]	$C_{10}H_{22}O_3$
Glushinskite	$MgC_2O_4{\cdot}2H_2O$
Guanine	$C_5H_3(NH_2)N_4O$
Hartite	$C_{20}H_{34}$
Hoganite	$Cu(CH_3COO)_2{\cdot}H_2O$
Humboldtine [38]	$(FeC_2O_4{\cdot}2H_2O)$
Idrialite	$C_{22}H_{14}$
Joanneumite [18]	$Cu(C_3N_3O_3H_2)2(NH_3)_2$
Julienite [18]	$Na_2Co(SCN)_4{\cdot}8H_2O$
Kladnoite [18]	$C_6H_4(CO)_2NH$
Kratochvílite	$C_{13}H_{10}$
Levinsonite-(Y) [18]	$YAl(SO_4)_2(C_2O_4){\cdot}12H_2O$
Lindbergite	$MnC_2O_4{\cdot}2H_2O$
Mellite [18]	$Al_2C_6(COO)_6{\cdot}16H_2O$
Moolooite	$CuC_2O_4{\cdot}nH_2O$
Oxammite [18]	$(NH_4)_2(C_2O_4){\cdot}H_2O$
Paceite	$CaCu(CH_3COO)_2{\cdot}6H_2O$
Paraffin hydrocarbon	
Sodium urate	$C_5H_3N_4NaO_3$
Stepanovite [18]	$NaMgFe(C_2O_4)_3{\cdot}9H_2O$

(continued)

Table 1 (continued)

Name	Formula
Tinnunculite [18]	$C_5H_4N_4O_3 \cdot 2H_2O$
Triazolite [18]	$NaCu_2(N_3C_2H_2)_2(NH_3)_2Cl_3 \cdot 4H_2O$
Urea	$CO(NH_2)_2$
Uricite	$C_5H_4N_4O_3$
Uroxite [18]	$[(UO_2)_2(C_2O_4)(OH)_2(H_2O)_2] \cdot H_2O$
Weddelite	$CaC_2O_4 \cdot 2H_2O$
Whewellite	$CaC_2O_4 \cdot H_2O$
Zhemchuzhnikovite [18]	$NaMgAl(C_2O_4)_3 \cdot 9H_2O$
Zugshunstite-(Ce) [18]	$CeAl(SO_4)_2(C_2O_4) \cdot 12H_2O$

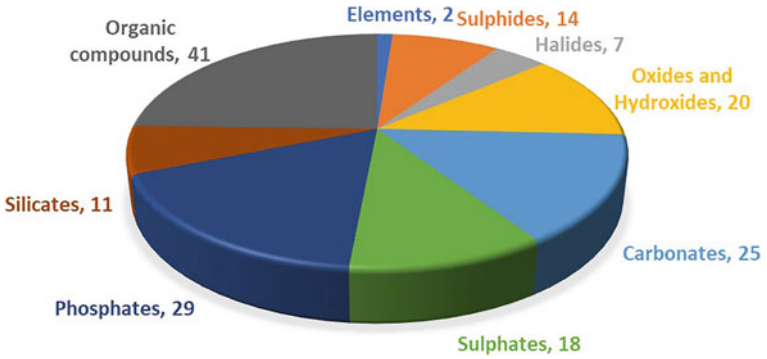

Fig. 1 Distribution of biominerals over Strunz classes

variable because they depend on many different factors and conditions that cellules can modulate to obtain the required biomineral structure and architecture.

2.1 Biologically Controlled and Induced Biomineralization

As previously mentioned, biominerals are classified based on the causative effect of cellular processes into two main classes [7, 12, 19]: biologically controlled mineralization (BCM) and biologically induced mineralization (BIM). In BCM organisms have extensive control over the mineral formation. BCM results in well-ordered mineral structures with minor size variations and species-specific crystal habits [39]. BCM can occur extracellularly or intracellularly. In the first case, the cellule fed ions to the mineralization area, generally the outermost cell wall, where a template, such as a biopolymer, drives the nucleation and subsequent particle attachment and biomineral formation (see e.g. so called "low magnesium" foraminifera, Fig. 2a–c). For intracellular BM, nucleation occurs within the cell, the nanocrystals are then fed to the area where the biomineral form (such as so called "high magnesium" or "porcelanaceous" foraminifera Fig. 2d–f). In BIM, organisms have no to minor control over the mineral formation. BIM generally results in heterogeneous mineral compositions with poor crystallinity, including large size variations, poorly defined crystal morphologies and the inclusion of impurities. Their formation is due to a change in bulk water chemistry related to cellular processes. Structures indistinguishable from BIM products can be also produced in the absence of organisms and highly organized minerals may form in the presence of organic abiotic substrates. Figure 2g shows an occurrence of "green rust" (a ferrous-ferric hydroxide) [40, 41], which is likely related to siderophore production and release, and results in the unexpected stabilization of ferrous iron during photosynthetic activity of bacteria. Red, muddy sediments in Fig. 2g are made of goethite, a ferric oxyhydroxide; the change from red to green sediments occurs at a length scale of tens of centimetres. This

is indicative of the typical spatial variability of microorganism's communities and functions and their capacity of building and differentiating microenvironments.

Analysis of morphological and structural properties can lead to the attribution of the mineralization to BIM and BCM. Frankel and Bazylinski [24] list most of the Fe and Mn BIM and these mainly involve extracellular deposition of minerals. However, there are several reports of intracellular deposition of minerals that seem to blur the border between BIM and BCM. For example, many bacteria have iron storage proteins known as bacterioferritins that compartmentalize iron at concentrations far

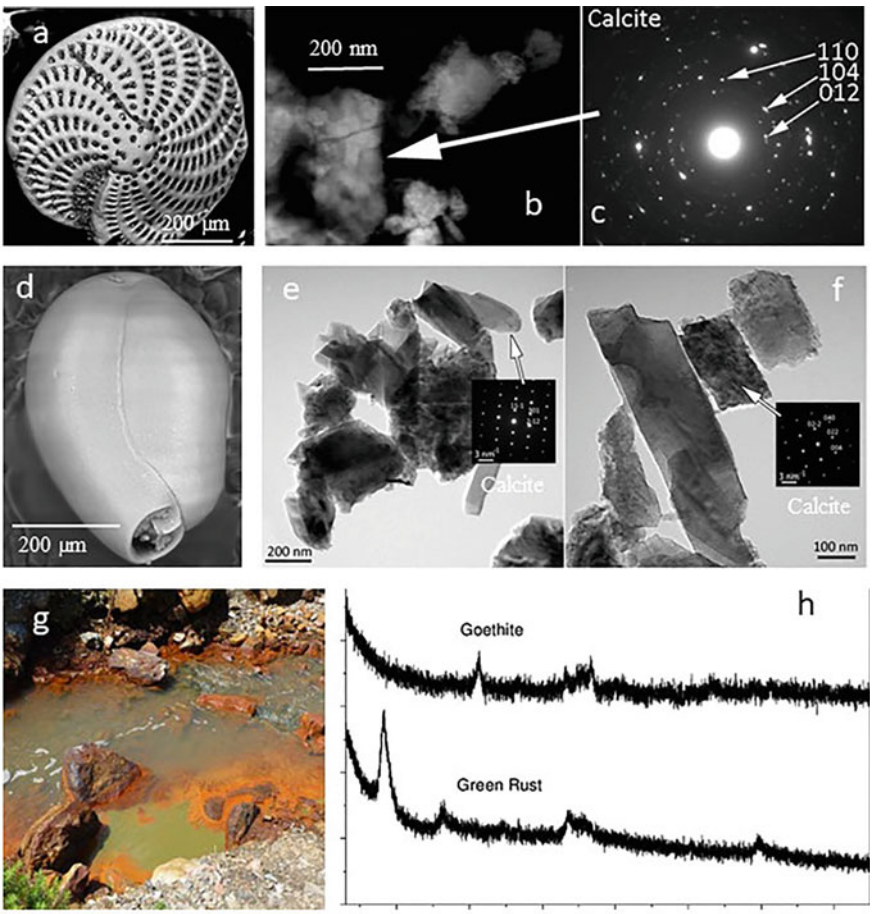

Fig. 2 **a**–**f** Images of Ca-carbonate biomineralizations: **a** SEM (scanning electron microscopy) image of extra-cellular BCM foraminifera *Elphidium*; **b** HRTEM image of a fragment and **c** selected area electron diffraction (SAED); **d** SEM image of intracellular BCM *Quinqueloculina* seminula; **e** and **f** HRTEM images with SAED of the calcite needles; **g** "green rust" occurring in a mine polluted river; **h** XRD patterns of the green sediments (bottom pattern) and the red sediments (top pattern) in (**g**)

above the solubility of Fe^{3+} [42]. Thus, attribution to BIM or BCM can be in some instances somewhat uncertain. For this reason, understanding biomineralization processes often requires the use of advanced investigation tools.

A strategy often adopted to understand the biomineralization process is to test the in vitro capability to drive mineralization of cultured cells, then the bio-mineralization effect of cell lysate and/or released polymers [43–45]. In this way, the role that in vivo cells, lysate of cell walls, and molecules released to the solution play on mineralization can be individually recognized allowing the attribution to BIM or BCM.

2.2 Mineral Surfaces and the Origin of Life

Since the original question about the physical origin of life [46] the scientific community has gained terrific insight into the complexity of life and its interaction with mineral surfaces interaction. Life functions through the specialized chemistry of carbon and water, and builds largely upon four key families of chemicals: lipids (cell membranes), carbohydrates (sugars, cellulose), amino acids (protein metabolism), and nucleic acids (DNA and RNA). Researchers generally think that current life descends from an RNA world, although other self-replicating molecules may have preceded RNA. There is a consensus that mineral surfaces play a pivotal role in biomineralization processes because they can favour selective adsorption of molecules and favour bio-polymerization processes. A large body of literature investigates how self-replicating molecules, or their components, came into existence. The role of minerals in polymerization of amino acids and nucleic acids, and the selective adsorption of organic species, including chiral molecules, onto mineral surfaces are two aspects of main interest for bio-mineral interactions.

A consistent body of experimental evidence suggests that vesicle-forming lipids and self-assembling lipid amphiphilic molecules [47] are at the base of the origin of life (see also [48], and references therein), in a step in which minerals may have played a useful, if not essential, role. However, besides self-assembling lipids, many of the key building blocks of life, including amino acids, sugars, and nucleic acid bases, are highly soluble in water and do not spontaneously self-organize. For these molecules, minerals may have provided a critical template for the formation of biopolymers.

Selective adsorption of organic molecules on mineral surfaces represents a viable mechanism for prebiotic molecular symmetry breaking. Chiral mineral surfaces abound in the natural world, and they have been shown to separate left- and right-handed molecules. Quartz is the only common chiral rock-forming mineral (i.e., it occurs naturally in both left- and right-handed crystals), but all centric crystals also have the potential to display chiral fracture or growth surfaces [49, 50], as well as chiral surface features such as steps and kink sites [51–53]. Common intrinsically chiral surfaces, in addition to those of quartz, include feldspar (110), clinopyroxene (110) and (111), olivine (111), clinoamphibole (110) and (011), calcite (214), and gypsum (110) and (111) faces.

Calcite is central to the origin of life in geochemically plausible origin scenarios because (1) calcite and other rhombohedral carbonate minerals were abundant in the Archean Era (e.g., [54, 55]); (2) calcite strongly adsorbs amino acids [19, 56–58]; (3) calcite's surface growth topology is dramatically affected by adsorbed L- versus D-amino acids [51, 53, 59–61]; (4) calcite scalenohedral (214) -type crystal faces demonstrated selective adsorption of D- and L- amino acids [52, 62, 63]. Through the co-evolution of life and minerals, deep modification occurred leading to the actual diversity of bio-mineral interactions.

The special role of clay minerals was advocated because these minerals have both high surface electrostatic charge and large reactive surface areas that facilitate the absorption of organic molecules. Clay minerals were found to concentrate and favour polymerization of amino acids to form small protein-like molecules [64] and can act as scaffolds in the formation of RNA, the polymer that carries the genetic message enabling protein synthesis [65–72]. Moreover, fine-grained clay particles may induce polymerization, though the molecular-scale mechanisms of the process are not yet fully understood [47].

DNA binding and conformation on mica surfaces as a function of solution compositions, has successfully been investigated by several means [73–75]. It is now well established that the DNA conformation on mica changes with cationic content and ionic strength, where a larger ionic potential (charge/density) favours adsorption. Valdrè et al. [76] pointed out that anisotropic surface properties of atomic-flat natural Mg–Al-hydroxysilicate substrate drives self-assembly and nanopatterning of nucleotides. RNA and DNA selectively adsorb on the surface of the Mg-hydroxide layer, with a higher concentration at the edge. No adsorption of RNA and DNA on surface of the TOT (tetrahedral–octahedral–tetrahedral sequence) layer was instead observed. Moro et al. [77] investigated interaction among di-glycine and clinochlore surfaces, showing preferential adsorption of di-glycine onto the hydrophobic brucite-like sheet, with the observed molecules organized as dot-like (single-molecules), agglomerates, filament-like and network structures by the surface, whereas only very few peptides were adsorbed onto the hydrophilic talc-like layer.

2.3 Biological Interfaces

Cellular membranes and cellular activity can modify physical properties of biological interfaces by effects on water dielectric properties, adding lipids and polysaccharides at the interface. In this way, cellular activity can exert a control on biomineralization kinetics, nucleation and growth regime, crystal size, crystal shape, and molecules aggregation [78]. These mechanisms explain the differences among mineral growth from aqueous solution, where growth regime dominates, and their biomineral analogue where nucleation regime generally dominates.

Regarding the role of water, it has become apparent that the interaction with water codetermines the molecular and supra-molecular organization of lipids and proteins within the cellular membrane ([79] and references therein). Membrane hydration

drives the self-assembly of the bilayers, and studies of partially hydrated bilayers by X-ray scattering, neutron scattering and calorimetry indicated that the fluidity of the lipid phase—an essential parameter for membrane function—varies strongly with the degree of hydration [80]. Inversely, NMR (nuclear magnetic resonance) experiments have shown that the lipid head groups have a strong influence on the local water structure [81–86]. Biomembranes are bilayers of mainly amphiphilic phospholipids, which are composed of a glycerol unit with two hydrophobic fatty acid "tails" and one hydrophilic phosphate ester "head group". The self-assembled nature of the lipid bilayer membrane makes it a complex and dynamic system, whose behaviour and properties strongly depend on composition and temperature.

Interface between cellules and mineral surfaces is the place where organic molecules are released by living organisms to exert their physic-chemical control on the surrounding environment, namely solution pH and Eh, partial pressure of CO_2, ionic strength and so on.

Several critical biochemical phenomena involve electron transport. For instance, sulphur reducing bacteria and metal reducing bacteria entail unique biomolecular machinery optimized for long-range electron transport. Microorganisms have adapted multiheme c-type cytochromes to arrange heme cofactors into wires that cooperatively span the cellular envelope, transmitting electrons along distances greater than 10 nm. Recently, the first crystal structure of a representative decaheme protein was solved, but the mechanism of electron conduction remains difficult to probe experimentally. Therefore, at the molecular level, how these proteins shuttle electrons along their heme wires, navigating intraprotein intersections and interprotein interfaces efficiently, remains a mystery thus far inaccessible to experiment. Breuer et al. [87] reveal an evolutionary design principle significant to an entire class of heme proteins involved in mediating electron flow between bacterial cells and their environment. Insights into this phenomenon are of great importance for biomineral interactions and open the way to a multitude of potential biotechnological applications.

2.4 Nanocrystals and Mesocrystals in Biominerals

Understanding nanocrystal aggregation is a milestone for biomineralization studies. External morphology, microstructure, and texture provide important evidence of attachment-based growth, although they alone do not prove formation by a particle-based growth process. In fact, such features can be misleading. For example, irregular or branched morphologies can form through dendritic and spherulitic growth mechanisms from solution at high degrees of supersaturation [88].

Pioneer work of Penn and Banfield [89] shed light on mechanism of oriented aggregation of TiO nanocrystals. Banfield et al. [90] investigated biomineralization products of iron-oxidizing bacteria by high-resolution transmission electron microscopy (HRTEM); they revealed an alternative coarsening mechanism in which adjacent 2- to 3-nm particles aggregate and rotate so their structures adopt parallel

orientations in three dimensions. Crystal growth is accomplished by eliminating water molecules at interfaces and forming iron-oxygen bonds. Self-assembly occurs at multiple sites, leading to a coarser, polycrystalline material. Point defects (from surface adsorbed impurities), dislocations, and slabs of structurally distinct material are created as a consequence of this growth mechanism and can dramatically impact subsequent reactivity. Meldrum and Cölfen [78] summarized the possible reaction paths for (bio)mineralization processes pointing out the many steps and activation energies needed to aggregate ions, form nanocrystals or droplets, perhaps from mesocrystals and eventually achieve macrocrystals. De Yoreo et al. [91] pointed out that pure oriented attachment rarely occurs, this implies very low (less than 10°) or no misalignment among nanocrystals, while nearly oriented attachment often occurs with higher misalignment. This occurs in cyanobacterial biomineralization [92, 93]. Crystallization by particle attachment of amorphous precursors has been demonstrated in modern biominerals across a broad phylogenetic range of animals, including sea urchin spicules [94], spines [95, 96], and teeth [97]; the larval shells [98] and nacre [99] of mollusks; zebrafish bone [100] and mouse enamel [101]; and scleractinian coral skeletons [102].

3 Minerals and Life: A Co-evolution History

Biominerals are widespread in nature because they allow an organism to have a protective internal or external structure and to support physiological functions. The mutual impact of life evolution on mineral diversity is well documented in the geological record, and the scientific community considers that life and minerals coevolved through the geological time [13, 103]. Calcium carbonates probably forms the most known biomineralizations and it is the major constituent of the biogenic mineral reservoir. Since the earliest times, bacterial activity has been a driving force in Ca carbonate formation [104], as demonstrated by stromatolite formation dating at least 3.48 Ga, even though the greatest diversity of stromatolites in Earth's history was recorded between 2.25 and 2.06 Ga, in the aftermath of the Paleoproterozoic glaciations [13, 105]. Stromatolites can show remnants of fossilized microorganisms and are likely the most ancient evidence for BM. Unfortunately, cellularly preserved fossils and palimpsest microstructures are present only rarely in ancient stromatolites and the attribution of ancient stromatolites to BIM or BCM is still debated. Clearcut BCM examples appeared at a later stage of the coevolution history.

3.1 Ca Carbonate Biominerals

The history of BCM in trilobites, the dominant marine arthropods that lived during the Palaeozoic, is well documented. Across the time from life explosion in the Cambrian to mass extinction in the Permian, trilobites developed at least nine different taxa and

three types of compound eyes, all with lenses supposed to consist mainly of primary calcite. The various kinds of trilobite eyes became highly diverse due to the demands provided by the various new environments.

Further examples of Ca-carbonate controlled biomineralization processes are offered by molluscs, clams, oysters, gastropods, foraminifera, coccolithophores, and corals (Fig. 3). These organisms developed the capability to select specific polymorphs, namely calcite, aragonite, vaterite, monohydrocalcite, and the amorphous calcium carbonate (ACC). These can occur, either singularly or together, in specific structures within an organism, or they may form sequentially during their development [8]. A typical case of phase transition was discovered in forming spicules in embryos of *Strongylocentrotus purpuratus* sea urchins. For instance, using X-ray absorption near-edge spectroscopy (XANES) and photoelectron emission microscopy (PEEM), [106] observed a sequence of three mineral phases: hydrated amorphous calcium carbonate ($ACC{\cdot}H_2O$) → ACC → calcite. Interestingly, $ACC{\cdot}H_2O$-rich nanoparticles can persist after dehydration and crystallization due to protein matrix components occluded within the mineral that inhibit $ACC{\cdot}H_2O$ dehydration. Weiss et al. [98] showed a similar function for ACC in the larval shells of the marine bivalves *Mercenaria mercenaria* and *Crassostreagigas*, where ACC transforms to aragonite.

In the last decades, it has been pointed out that the evolution of life implies adaptation to minerals, and this is genetically encoded in the organism's cellules. With life development across the geological record, biomineral numbers and type increased to support the different actual functions. Carbonate precipitation mediated by bacteria can occur as a by-product of metabolic activities (photosynthesis, ureolysis, denitrification, ammonification, sulphate reduction, and methane oxidation) that induce chemical variations at the microorganism-solution interface.

Other reported bacterial carbonate biominerals are rhodochrosite [113], hydrozincite [114], siderite [115], etc. More details on bacterial biomineralization can be found in the "Waters, metals and bacterial mineralization" paragraph.

3.2 Ca Phosphate Biominerals

The occurrence of Ca phosphate biominerals has been observed in living creatures from unicellular organisms to vertebrates [7, 116]. Bones are the most relevant example of phosphate biomineral in vertebrates. They are made up of a combination of inorganic calcium phosphate and an organic matrix. The inorganic phase comprises ~60–70% of the total bone mass [117] and consists of a nanocrystalline carbonate-hydroxyl-apatite (CO_3^{2-} at ~4.5 wt%). The remaining mass is formed by an organic matrix (20–30%, collagen fibres, glycoproteins and mucopolysaccharides) and water (10%). The combination and organization of the inorganic and organic components confers to the final material peculiar physical and mechanical properties providing toughness, the ability to withstand pressure, elasticity and resistance to stress, bending and fracture pressure [118].

Fig. 3 Images of Ca-carbonate biomineralizations: **a** mollusc shells (from Boettiger et al. [107], Copyright (2009) National Academy of Sciences); **b** Red Sea *Tridacna maxima* with its mantle exposed (from Lim et al. [108], Copyright (2020) Lim, Rossbach, Geraldi, Schmidt-Roach, Serrão and Duarte, under the Creative Commons CC BY license; **c** underwater photograph of coral reef in Indonesia with almost 100% cover of *Acropora* sp. (from Lesser [109], Copyright (2004), with permission from Elsevier); (d) coccolithophore species *Emiliania huxleyi* (from Triantaphyllou et al. [110], Copyright (2018) Triantaphyllou et al., under the Creative Commons Attribution License); **e** and **f** light micrographs of the foraminifera *Ammonia* sp. and *Haynesina germanica* from the Atlantic French coast intertidal mudflat and the Gullmar fjord (from LeKieffre et al. [111], Copyright (2018), with permission from Elsevier; **g** the pearl oyster *Pinctada fucata* (from Du et al. [112]), under the Creative Commons CC BY license

Bone constituents are highly hierarchically organised. Fibrillar collagen type I is the main component (∼90%) of the organic fraction [117]. At the molecular level, the polarized triple helix of tropocollagen molecules is grouped in microfibres, and carbonate-hydroxyl-apatite crystals nucleate and grow within small cavities between their edges. Microfibres combine in larger fibres that represent the microscopic units of bone tissue. Finally, large fibres are arranged in different structural distributions to form the full bone [118]. Bone formation takes place by controlled nucleation and growth through an extracellular process. The inorganic mineral component and the organic matrix are linked to each other at the molecular level as Ca^{2+} is bonded to phosphoproteins along the collagen fibres at regular intervals, following the inorganic crystal structure of apatite [118]. The crystallographic axis c of bone crystals is not random oriented, but it is arranged in parallel to the collagen fibres and to the largest dimension of the platelet, while a- and b-axes are aligned along two other dimensions. Bone crystals are characterised by a hexagonal crystal structure, and they are 2–6 nm thick, 30–50 nm wide, and 60–100 nm long. The carbonate ions can substitute both phosphate (B-type substitution) and hydroxyl ions (A type substitution) in the lattice [116, 117]. The presence of carbonate ions and minor ions such as Mg^{2+}, Na^{+}, K^{+}, Cl^{-} and F^{-} leads to significant modifications in the lattice parameters with respect to purely inorganic apatites [118].

3.3 Fe Biominerals

Iron, together with Ca and Mg, is the most widespread metal in biominerals, due to Fe abundance on Earth, and to its important role in many metabolic processes. Bacteria represent the major mediators in the deposition of Fe biominerals in a host of different environments [8]. Iron biominerals allow organisms to accumulate the metal for future metabolic needs, avoiding high intracellular accumulation [119]. Other properties of Fe biominerals, potentially useful to organisms, include hardness, density and magnetism [119]. The ferric hydroxides or oxyhydroxides are an important class of Fe biominerals and can occur as amorphous or low-crystalline precipitates, such as ferrihydrite ($Fe_{4–5}(OH,O)_{12}$), or as crystalline phases such as lepidocrocite (g-FeO(OH)) or goethite (α-FeO(OH)) [33, 119, 120]. The Fe oxide magnetite, Fe_3O_4, is another important Fe biomineral. Magnetite is characterised by magnetic properties, high density (5.1 g/cm^3) and hardness. Uniformly sized particles of magnetite, often arranged in chains, are formed by magnetotactic bacteria allowing them to align according to the Earth's magnetic field [121]. Magnetite also occurs in the radular teeth of chitons, flattened molluscs, commonly found on hard substrata in intertidal regions of coastlines around the world ([122, 123] Fig. 4a–d). In chiton teeth, mineralization occurs within an organic matrix (α-chitin and protein) through several steps to form mature teeth, and chitons possess all stages of tooth development in one radula [124]. Specifically, four stages have been observed: (i) newly secreted unmineralized and transparent teeth, composed of α-chitin and proteins, and Fe transportation into the organic matrix; (ii) heterogenous nucleation of ferrihydrite

on acidic proteins coating the alpha-chitin fibers; (iii) solid-state transformation ferrihydrite → magnetite; (iv) fully mineralized teeth in both shell and core (the tooth core region is filled, [124]) (Fig. 4d, [125]). The deposition of these composite structures, refined by evolution over millions of years, confers unique properties to the chiton teeth, such as tensile strength, shock absorption and controlled wear and abrasion, resulting in highly efficient feeding tools [123, 126].

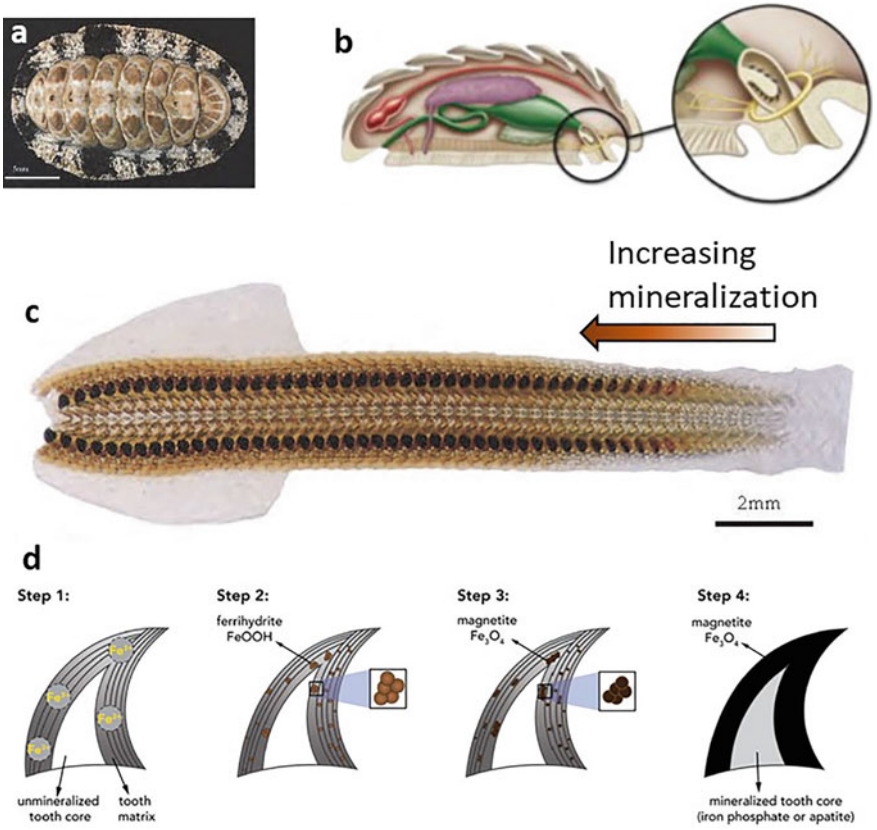

Fig. 4 Chiton, chiton teeth and their formation. **a** Chiton (*Acanthopleura gaimardi* species characterized by eight overlapping aragonite plates surrounded by a fleshy girdle covered by small aragonite spines) (from Brooker and Shaw [123], Licensee IntechOpen, under the terms of the Creative Commons Attribution 3.0 License); **b** internal anatomy of a representative chiton showing the location of the radula, a rasping, toothed conveyor belt-like structure used for feeding (from Weaver et a. [127]), Copyright (2010), with permission from Elsevier); **c** optical micrograph of the radula of *Acanthopleura gaimardi*; the arrow indicates the progressive stages of radular tooth development (from Brooker and Shaw [123], Licensee IntechOpen, under the terms of the Creative Commons Attribution 3.0 License); **d** hypothesized mechanism of Fe biomineral formation (ferrihydrite and magnetite) in chiton teeth (see text for explanation) (from Moura and Unterlass [125], Licensee MDPI, Basel, Switzerland, under the Creative Commons Attribution)

4 Geo-Bio Interactions and the Environment

4.1 Biofilm Composition and Structure

Most bacteria in the environment live associated with surfaces, in so called biofilms [128, 129]. Biofilms are the oldest form of life recorded on Earth [130] documented by petrified biofilms in Precambrian stromatolitic rocks [131]. They occur in nearly every moist environment where sufficient nutrient flow is available and surface attachment can be achieved [132, 133]. Biofilms can be formed by a single bacterial species, although they often consist of many species of bacteria, fungi, algae and protozoa that are attached to abiotic surfaces, such as minerals and rocks, or air–water interfaces, and to biotic surfaces, such as plants, roots, leaves and other microbes. Attachment is favoured on surfaces that are rough, hydrophobic and coated by surface conditioning films [128, 132], and are widespread both in subaerial and in subaquatic environments. Also, biofilms can grow in extreme environments characterised by extreme temperature, extreme pH values, high salinity, high pressure, poor nutrients, etc. Microorganisms that can survive in these extreme environments are called extremophiles [134], which include thermophiles, alkaliphiles, acidophiles, halophiles etc. according to the harsh condition that characterises the specific environment.

In this chapter, biofilm formation mechanisms and characteristics will be discussed briefly; for excellent comprehensive reviews on this topic see O'Toole et al. [135], Hall-Stoodley and Stoodley [136], Verstraeten et al. [137]. Biofilm matrix consists mainly of water (79–95%), which is held by the highly hydrated extracellular polymer substances (EPS), that represent 70–95% of the organic matter of the dry mass of the biofilm. The microorganisms are only a minor part of mass and volume but exert an important role by excreting the EPS and controlling the physical and chemical properties of biofilms [131, 138–140] (see Table 1 in Flemming and Wingender [141]). EPS are a complex mixture of highly hydrated biopolymers mainly consisting of polysaccharides, as well as proteins, nucleic acids, lipids and humic substances, which keeps the biofilm cells together. In Gram-negative cells, the EPS are made up of lipopolysaccharides, capsule polysaccharides, excreted polysaccharides and proteins; in Gram-positive cells, the main component of the EPS are lipoteichoic acids, polysaccharides and proteins [142]. EPS chemical composition and structure vary depending on the type of substrate upon which the cells are grown and are affected by environmental stress [128, 142, 143].

The development of a biofilm occurs, firstly, through cell attachment by physicochemical interactions or extracellular matrix protein secretion to form a cell monolayer, this stage is followed by biofilm maturation and, finally, detachment of cells. Biofilms can be highly organized, and can form a single layer, a three-dimensional structure or even aggregates [144]. For subaquatic biofilms, the structure changes according to water flow conditions. In fastmoving waters, biofilms tend to form filamentous streamers (e.g., drainage run-off from acid mines, hydrothermal photosynthetic mats), whereas in quiescent waters, biofilms form mushroom or mound-like

structures characterised by isotropic overall patterns, similar to those of stromatolites [128].

Biofilms actively interact with elements in waters (subaquatic biofilms) and with the attachment surface (subaerial and subaquatic biofilms). In the following paragraphs biofilm-metal interactions in aquatic environment and the influence of biofilms on the attachment surfaces will be presented.

4.2 Biofilm-Metal Interaction in Aquatic Environments

In aquatic environments, trace elements interact with biofilms through physical, chemical and/or biological processes [145–147]. Metal distribution, immobilisation and remobilisation will depend mainly on (i) the sorption properties of the biofilm, (ii) the type and concentration of the ligands within the biofilm matrix, (iii) the pH values and redox potential conditions at the cell/EPS surface, (iv) the physico-chemical characteristics of waters, and (v) the availability of reactive mineral surface sites (e.g. oxide, sulphide, phosphate, carbonate precipitates) ([145] and references therein). It has been demonstrated that low pH values favour the release of ions from a bound state, due to the competition with H^+ ions, while high pH values tend to favour their chelation. For example, Ferris et al. [148] grew microbial biofilms in acidic (pH 3.1) and near neutral water contaminated with metals from mine wastes, and they observed that biofilm metal uptake at a neutral pH level was enhanced by up to 12 orders of magnitude over acidic conditions. Moreover, adsorption strength values were usually higher at elevated pH levels.

Metal uptake occurs mainly through ion exchange, chelation, adsorption, and diffusion through cell walls and membranes [145], and it has been observed that EPS play an important role in the sorption of metals in biofilms due to the presence of anionic groups such as carboxyl, phosphoryl, and sulphate groups [142] that allow the formation of unidentate, bidentate and multidentate complexes of cations with anionic groups on the EPS molecules [145].

Both living and dead cells can accumulate metals through metabolism-independent association with cell walls and other external surfaces. Metabolism-dependent transport across the cell membrane and transport systems occurs only in living cells [149]. In the first mechanism, metal binding on cell walls is affected by their structure. In Gram-positive bacteria, the cell wall is composed of an intermingling of peptidoglycan and secondary polymers. Peptidoglycans consist of polysaccharide chains cross-linked by oligopeptides. Carboxylate groups at the carboxyl terminus of individual chains provide the bulk of the anionic character of peptidoglycans [146, 150]. Other secondary polymers include teichoic acids and teichuronic acids, which contain phosphate and carboxylate residues, respectively. Peptidoglycan and the cell wall acids are exposed to the external aqueous solution and form the surface of the bacterial cell. The anionic functional groups present in the peptidoglycan, teichoic acids and teichuronic acids of Gram-positive bacteria are the main components responsible for the anionic character and metal binding capacity of

the cell wall [151]. In Gram-negative bacteria, cell wall is characterised by a more complex structure made up of (i) an outer porous and highly permeable membrane, rich in protein and lipopolysaccharide, (ii) a thin layer of peptidoglycan, enzymes and structural proteins in the periplasmic space. The peptidoglycan, phospholipids, and lipopolysaccharides are the primary components involved in the metal binding in Gram-negative bacteria. On the surface of bacteria, a well-ordered layer (S-layer), made up of protein and glycoprotein subunits, is frequently observed. Here, exposed anionic residues can react with dissolved metals [150, 151].

Metabolism-dependent transport of metals may be a slower process than biosorption on the cell wall, and can be affected by the temperature, the absence or presence of an energy source, the physiological state of cells and the nature and composition of the growth medium. Metals transported into the cell may be bound, precipitated, localized or translocated to specific intracellular structures or organelles depending on the metal and the bacteria species [152]. Passive biosorption and metabolic uptake can occur in the same bacteria species. Gourdon et al. [153] isolated Gram-positive and Gram-negative bacteria from activated sludge to evaluate Cd biosorption. At 30° and pH 6.6, Cd biosorption was higher (20%) in Gram-positive bacteria than Gram-negatives. This difference was attributed to the cell wall composition, rich in glycoproteins in the Gram-positive bacteria. These are characterised by a higher number of potential binding sites for Cd than phospholipids and lipopolysaccharides that characterised the external layer of the cell wall in Gram-negative bacteria. Biosorption was mainly attributed to the interaction of the metal with the bacteria surfaces, although metabolic uptake appeared to occur, especially in Gram-positive bacteria.

The sorption of pollutants on biofilms can be considered a dynamic process because biofilms are not chemically inert, and variations in environmental conditions can affect the microbiota and their physiology. Moreover, the detachment of biofilms can lead to microbial degradation processes of the biological binding sites, resulting in remobilization of metals, thus representing a secondary source of contaminants [154].

4.3 Waters, Metals and Bacterial Mineralization

In aquatic environments, bacteria are ubiquitous microorganisms that can precipitate a wide range of authigenic minerals, and drive both modern and ancient biogeochemical cycles from the microenvironment to global scales [155]. Indeed, bacteria have a remarkable potential to sequester and accumulate cations onto their surfaces mainly because (i) cell walls are ionized and naturally anionic (pH between 5 and 8), and because (ii) they are characterised by a large surface area to volume ratio due to their small size. Transition metals, due to their electronegativities, oxidation state, hydrated radii and hydration energies [156], are characterised by an extremely high affinity for the polymeric material present in the cell wall and outer membrane (carboxyl and phosphoryl groups), and in the surrounding capsules (carboxyl and

hydroxyl groups) [157, 158]. During bacterial biomineralization, often, metals are electrostatically bound to the anionic surfaces of the cell wall and organic polymers, reducing the activation energy barriers to nucleation and providing sites for crystal growth [155, 159].

Due to its high concentration in natural waters compared to other trace metals [160], Fe is commonly bound to organic sites forming the greatest number of biominerals in waters (Fig. 5a, b). The microbial precipitation of Fe hydroxide is widespread in several aquatic systems, such as acid mine drainage environments, river sediments, deep subterranean groundwater, marine sediments, around deep-sea vents and in hydrothermal plumes [155] and references therein). In oxygenated waters, bio-Fe-hydroxides are commonly precipitated through different processes: (i) the binding of dissolved ferric species to negatively charged polymers, (ii) the reaction of soluble ferrous iron with dissolved oxygen and subsequent precipitation of ferric hydroxide on bacteria, and (iii) as a consequence of the metabolic activity of Fe^{2+} oxidizing bacteria that can induce ferric hydroxide precipitation as a secondary by-product [155]. *Acidithiobacillus ferrooxidans* and *Leptothrix* sp. are common microorganisms that produce Fe^{3+} sheaths and can be responsible for the production of copious amounts of Fe^{3+} mineral phases in the environment [161]. These bacteria utilize the oxidation of Fe^{2+} ions by O_2 as a source of energy [8, 119]. Ferric hydroxide can then evolve in more stable Fe oxides (e.g., hematite and goethite) via dehydration or dissolution–reprecipitation. Some peculiar bacteria, magnetotactic bacteria, can precipitate magnetite and greigite whose crystals are arranged in chains enclosed in membrane vesicles (magnetosomes) [119, 155]. The abundance and morphology of magnetosomes can reflect environmental conditions and they have been used as paleoenvironmental proxies as reported by He et al. [162].

Silica [163, 164], phosphate [165], carbonate [16], and sulphate/sulphur [166] available in solution may react with Fe bound to bacterial surfaces to form other authigenic mineral phases [161, 167]. The final product will depend on both the control of the bacteria on the precipitation process and on the pH values and redox conditions of the specific environment. For example, [165] investigated the depth variations of Fe and P speciation in Lake Pavin (Massif Central, France), by applying complementary research techniques such as X-ray diffraction (XRD), scanning electron microscopy (SEM), (HR)TEM (high resolution - transmission electron microscopy), synchrotron-based scanning transmission X-ray microscopy (STXM) and XANES at the Fe $L_{2,3}$-edges and the C K-edge. They found that Fe is hosted in different mineral phases: (i) in the shallower oxygenated water column (25 m), Fe is mainly hosted by Fe(III)-(oxyhydr)oxides and phyllosilicates, (ii) close to the chemocline (at 56 m depth), an additional amorphous Fe(II)–Fe(III)-phosphate phase was detected, (iii) in the deeper anoxic water (67 m and 86 m depths), vivianite ($Fe(II)_3(PO_4)_2{\cdot}8(H_2O)$) becomes dominant. A significant fraction of vivianite was observed at the surface of bacterial cells. Comparing field study with laboratory experiments, they proposed that Fe-oxidation may play a role in the precipitation of Fe-phosphates in the water column. Polyphosphate-accumulating microorganisms could also be involved in Fe-phosphate formation in the lake, by increasing dissolved phosphate concentrations in the monimolimnion. Both mechanisms play an important role in Fe and P cycling in

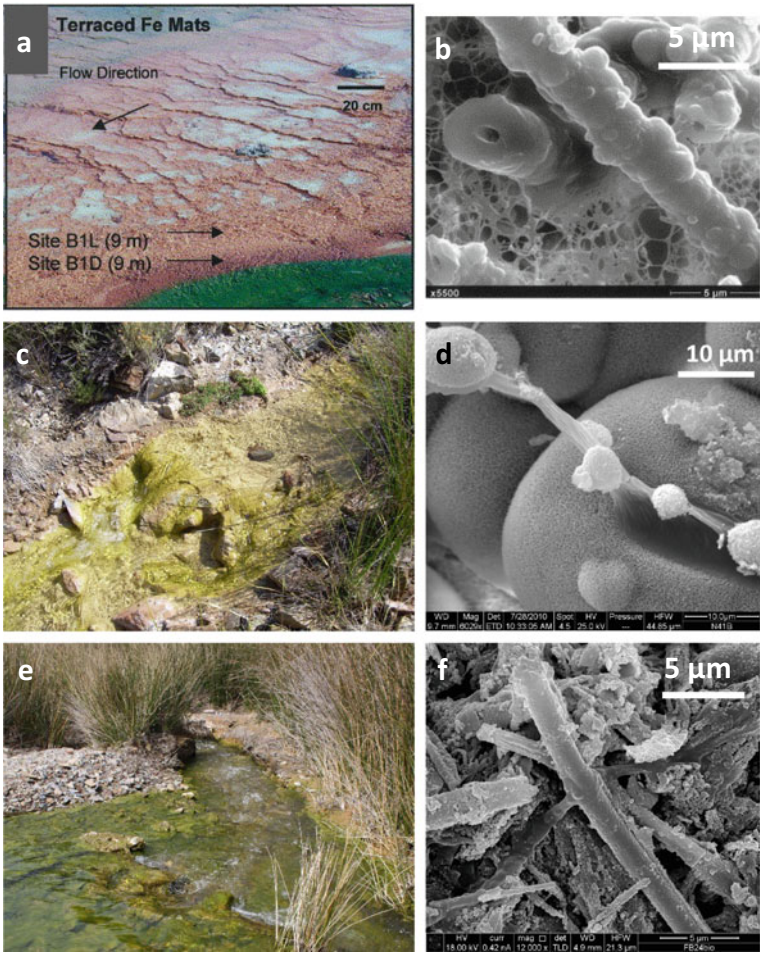

Fig. 5 Examples of bacterial biomineralizations: **a** Fe microbial mats at the Beowulf Spring located in Norris Geyser Basin, Yellowstone National Park; **b** SEM image of the filamentous As-rich Fe sheaths in the microbial mats; **a** and **b** from Inskeep et al. [161], modified, Copyright (2004), with permission from Elsevier; **c** and **e** microbial mats along the Naracauli stream responsible for formation of hydrozincite and amorphous Zn-silicate, respectively; **d** and **f** SEM images of hydrozincite and amorphous Zn-silicate, respectively

the investigated system. Along the Speed River (Ontario, Canada), Konhauser et al. [164] observed by TEM-EDS (energy dispersive spectroscopy) bacteria attached to different substrates and mineralized by Fe-rich capsular material to fine-grained (<1 µm) authigenic mineral precipitates. The authigenic grains are characterised by a wide range of morphologies, from amorphous gel-like phases to crystalline phases. The most abundant mineral is a complex (Fe, Al) silicate of variable composition. The gel-like phases are chemically similar to a chamositic clay, whereas

the crystalline phases are more siliceous and have compositions between those of glauconite and kaolinite. The adsorption of dissolved constituents from the aqueous environment contribute significantly to the transfer of elements to the streambed sediments, considerably affecting the biogeochemical cycle of Fe, Si and Al. Ferric hydroxide and ferric hydroxysulfate precipitation by bacteria was observed by [166] in acid mine drainage lagoon sediments. TEM-EDS analysis revealed that bacteria are characterised by Fe-rich capsules, and Zn, Ti, Mn and K are incorporated into the mineralised matrix. In the subsurface, cells are associated with granular, fine-grained mineral precipitates, composed almost exclusively of Fe and S.

The type of bacterial biomineral is affected by the available ions in waters in which the microorganisms are growing [155, 167, 168], leading to a great variety of biomineralization patterns. In the Carnoulès AMD (acid mine drainage), Benzerara et al. [169] investigated As biomineralization by TEM, STXM, and near-edge X-ray absorption fine structure (NEXAFS) spectroscopy at the C K-edge, Fe $L_{2,3}$-edge, and As $L_{2,3}$-edge. Authors observed isolated spheres of Fe–As–S-rich precipitates (tooeleite and an amorphous phase) agglomerating outside the bacterial cell wall and forming, in some cases, thick continuous layers around the cells. Arsenic biomineralizations have been observed also in geothermal systems as reported by Tazaki et al. [16] and Inskeep et al. [161]. On the walls of the drainage systems of Masutomi Hot Springs (Yamanashi Prefecture, Japan), some bacteria accumulate Fe and As along with other trace elements to form various biominerals on the surface of the cell: hydrous iron oxides, calcite and lollingite ($FeAs_2$). Fourier-transform infrared spectroscopy (FT–IR) revealed the presence of organic components such as C—H, C = O, CNH, –COOH, and N—H, emphasizing the metal-binding potential of the bacteria [16]. Authors suggested that the polysaccharides of the bacteria may initially adsorb H_4SiO_4 and Ca ions from the spring water to form a mineral complex containing calcite. Then, Fe–As adsorption takes place through the cohesion of spherules, and finally lollingite precipitates over the calcite that encapsulated the bacterial cell surfaces.

Peculiar examples of bacterial biomineralizations occur along the Naracauli stream which drains the abandoned mining site of Ingurtosu (SW Sardinia, Italy). Specifically, at two distinct locations along the stream, bacterial activity drives the precipitation of two different Zn biominerals. At one location, in late spring-early summer, bioprecipitation results in the formation of hydrozincite ($Zn_5(CO_3)_2(OH)_6$), in association with a photosynthetic community including the cyanobacterium (*Scytonema* sp), and the microalga (*Chlorella* sp) [14] (Fig. 5c). Bio-hydrozincite precipitates on different substrates such as rocks, plant roots or stems on which the biofilm can adhere. SEM analysis (Fig. 5d) showed the association of the Zn hydroxycarbonate with the biological matrix such as bacterial sheaths, and extracellular polymeric substances. XRD and HR-TEM analysis indicated that, in comparison to abiotic hydrozincite, bio-hydrozincite is characterised by higher content in lattice defects (e.g., grain boundary, line defects), and by a higher a_o lattice parameter presumably reflecting differences in the stacking sequence of tetrahedral–octahedral–tetrahedral (TOT) units that are held together by distorted carbonate groups [114, 170] in the hydrozincite structure. Bio-hydrozincite is characterised by the

presence of nanocrystals that aggregate according to an imperfect aggregation mechanism to form mesocrystals [93]. Further downstream, in summer, a colloidal Zn-silicate biomineralization occurs in association with the bacterium *Leptolyngbya frigida* [30] (Fig. 5e). The biomineral is made up of nanoparticles that precipitate on bacterial sheaths forming microtubules that are embedded in extracellular polymeric substances (Fig. 5f). ^{29}Si magic angle spinning and ^{29}Si/^{1}H cross polarization magic angle spinning analysis, FTIR and XAS analysis revealed a poorly crystalline phase closely resembling hemimorphite ($Zn_4Si_2O_7(OH)_2 \cdot H_2O$), a zinc sorosilicate [31, 171].

The reported examples suggest that bacteria can control biotransfer processes and biogeochemical cycles in different environmental conditions. They are able to concentrate heavy metals and metalloids through different mechanisms, such as adsorption, complexation, and active transport into the cell, that are influenced by external physicochemical parameters, such as the pH and ionic composition of the host water [16]. Bacterial biomineralizations in the aquatic environments contribute significantly to decrease metal dissolved in solution, offering clues to possible methods of bioremediation. Also, their metal-binding capacity makes these microorganisms potential candidates in biorecovery [172] of economically valuable metals [155].

4.4 Soils, Metals and Plant Activity

The advent of land plants, about 400 million years ago, contributed to alter Earth's surface appearance and to increase the rate of clay mineral production of at least an order of magnitude greater than the previous eras, favouring the production of soils [13, 103, 175–177]. Indeed, leaching through roots causes incongruent weathering of primary to secondary minerals, promoting the formation of clay-sized layer silicates and different oxides and hydroxides of Fe, Al, and Mn [178]. Fungi can cooperate with plants favouring mineral weathering [179, 180], although the precise mechanism by which mycorrhizae alter minerals is poorly understood. Recent ultramicroscopic and spectroscopic studies by Bonneville et al. [175] demonstrated that biotite weathering by fungi can occur through a biomechanical-chemical process, starting by physical distortion of the lattice structure of biotite and subsequent dissolution and oxidation reactions that lead to mineral neoformation (vermiculite and clusters of Fe(III) oxides). Furthermore, the action of plant activity has strongly influenced biogeochemical cycles of major and trace elements [1, 181]. Conley [182] reported that biogenic silica (phytoliths) that precipitates in living tissues of growing plants is characterised by an annual production of 60–200 Tmole Si yr^{-1}, a value comparable in magnitude to the oceanic production of biogenic silica by diatoms, silicoflagellates, and radiolarians (240 Tmole Si yr^{-1}, [183]). Phytoliths represent a sizable pool of Si [184–186] that remains in the soil after decomposition of organic material together with other biogenic detritus.

Another example of coevolution of life and minerals is offered by mycorrhizae, since their appearance, these symbiotic associations support plant roots in mobilizing phosphorous and other nutrients from soil minerals. As this process favours plant growth, it resulted in increasing the size of plants, forest development, formation of thick soil layers and, ultimately, increasing the number of clay minerals [13, 103, 173]. Nutrients mobilizing functions are also provided by soil microbial communities where bacteria and fungi act symbiotically [174].

The rhizosphere is the narrow region of soil that is directly influenced by root secretions and associated soil microorganisms [187], and it is characterised by processes that are dramatically different from those that occur in the bulk soil [188, 189]. Here plant roots exert a critical role to regulate nutrient availability and to detoxify undesirable metal pollutants by realising a large number of metabolites that change the pH or form metal–metabolite complexes [190]. The secreted compounds consist of a complex mixture of inorganic ions (H^+, HCO_3^-), gaseous molecules (CO_2, H_2), low-molecular-weight compounds (organic acids, amino acids, phenolics and sugar) and high-molecular-weight compounds (mucilage, polysaccharides, and ectoenzymes) [189–191]. Organic chelating anions have a significant influence on the nucleation reactions, transformations, morphology, and surface properties of soil precipitates. Violante and Caporale [189] reported that in the presence of organic ligands the specific surface and reactive sites of Al and Fe precipitates increase, and they can lead to the precipitation of short range ordered precipitates (ferrihydrites, noncrystalline Fe and Al oxides, poorly crystalline boehmite (AlOOH)) instead of well crystallized Fe or Al oxides (gibbsite, goethite, hematite, lepidocrocite) that precipitate in the absence of organic ligands.

To survive in metal-extreme environments, plants have developed different tolerance strategies. In metal-hypertolerant plants, exudation of organic acids has an important role in metal (e.g. Cd, Al, Ga, Cu, Mn, Zn and Pb) detoxification mechanisms, because chelators form stable complexes with metals limiting their absorption and/or translocation by plants, maintaining low levels of contaminants in the aerial parts [190, 192, 193]. The uptake of potentially toxic metals and/or metalloids may be also reduced by formation of (bio)mineral precipitates at the soil-root interface. Iron plaques (e.g. ferrihydrite, goethite, lepidocrocite, siderite, etc.), whose mineral composition is depends on the local biogeochemical factors at specific sites, have been observed on the roots of many aquatic and wetland plants (e.g. rice roots) [112, 194, 195] (Fig. 6a). Some researchers suggest that Fe plaques can act as a barrier because a significant amount of metals (e.g. Cr, Pb, Cu, Zn) bind to them by complex formation [196, 197] (and references therein) (Fig. 6b). A similar mechanism has been observed in *E. pithyusa* [198] and *P. lentiscus* [199] by SEM, STXM and Zn K-edge X-rays adsorption fine structure (XAFS) spectroscopy. These plant species uptake Zn and Si from soil minerals and precipitate an amorphous Zn-silicate at the soil-root interface. This rim acts as a physico-chemical barrier against metal stress, and its formation was interpreted as intrinsically biologically driven (Fig. 6c, d).

If uptake of metals occurs, the plants can manage excess of toxic elements mainly by the following tolerance mechanisms: (i) sequestration/compartmentalization, (ii)

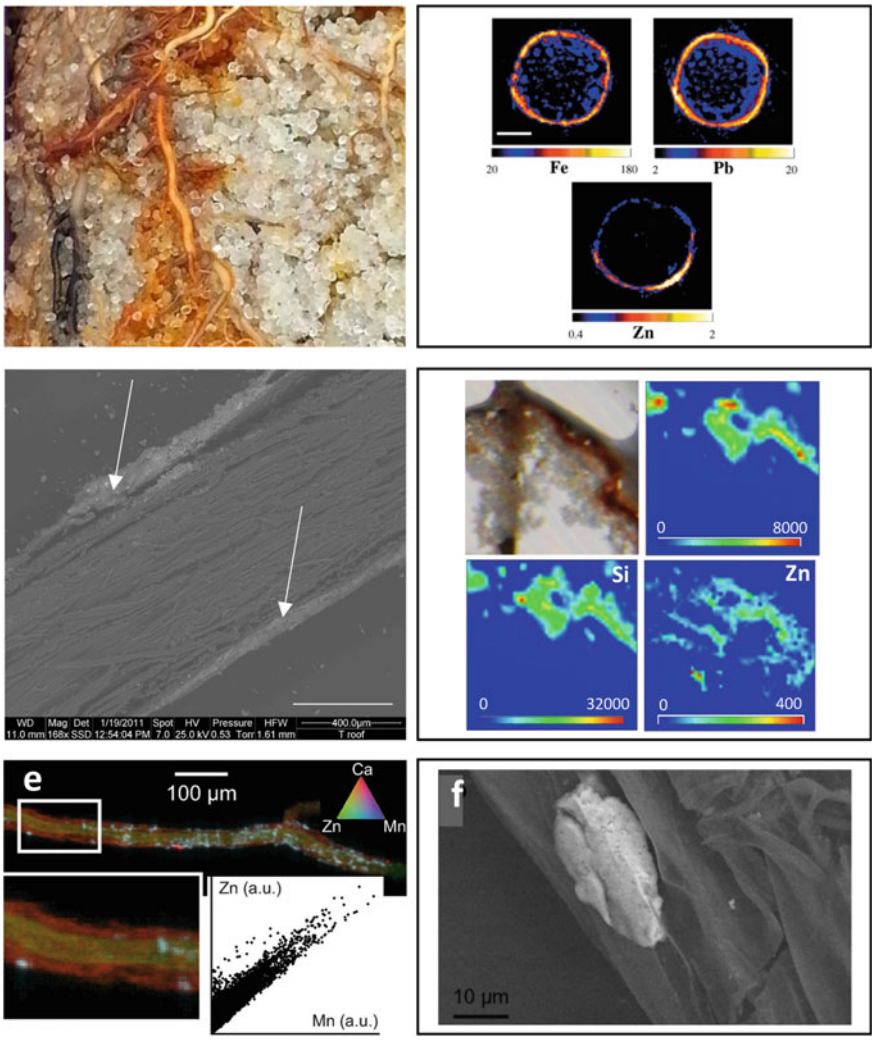

Fig. 6 Examples of plant biomineralizations. **a** Iron plaque formation at the rhizosphere-root interface of the wetland plant *Sparganium Americanum,* recovered from microcosm experiments (from Chang et al. [195], Copyright (2014) American Chemical Society); **b** fluorescence microtomography showing Fe, Pb and Zn distributions on and within roots of *Phalaris arundinacea* (scale bar, 150 µm) (from Hansel et al. [197], Copyright (2001) American Chemical Society); **c** SEM image of a *P. lentiscus* root (longitudinal section). The white arrows indicate the biomineral rim; **d** ordinary light stereomicroscope image of a thin cross root section of *E. pithyusa*, and LEXRF (low-energy X ray fluorescence) maps of Al, Si, and Zn (size of 80 µm × 80 µm, scan of 80 pixels × 80 pixels); **e** tricolor (RGB) µ-XRF map of a root of *Festuca rubra* grown on a Zn-contaminated sediment with Mn–Zn precipitates. Pixel size: 7 × 7 μm^2. The graph is a pixel-by-pixel scatterplot (Zn counts vs. Mn counts) that shows the constant Zn:Mn ratio; **f** scanning electron microscope image with backscattered electrons of Mn–Zn precipitates observed in the root epidermis of *Festuca rubra.* **e** and **f** from Lanson et al. [207], Copyright (2008), with permission from Elsevier

binding/chelation, (iii) excretion from aerial plant parts, (iv) enzymatic and non-enzymatic antioxidants, (v) protection, stress recovery and repair of damaged proteins [192, 200] (and references therein), and (vi) biomineral precipitation [26, 201–203]. In the binding/chelation mechanism, metals are bound/chelated by several metal-binding molecules such as organic acids, amino acids, and phenolic compounds and/or by metal-binding peptides, such as metallothioneins and phytochelatins, resulting in low metal concentrations in the cytoplasm [192]. As stated above, metal stress can also lead to the excretion of harmful elements from aerial plant parts. For example, McNear et al. [204], by synchrotron-radiation based X-ray fluorescence and absorption-edge computed microtomographies, found that, in the Ni-hyperaccumulator *Alyssum murale*, Ni and Mn are colocalized at the trichome base throughout the entire leaf contributing significantly to metal detoxification and compartmentalization. Tobacco (*Nicotiana tabacum* L. cv Xanthi) plants [205], exposed to toxic levels of Zn, can precipitate Zn-containing biogenic calcite and other Zn-containing compounds on the head cells of trichomes and subsequently they are excreted to alleviate metal stress. Other plant species, such as birch and willow, shed their leaves in autumn together with the load of potentially toxic elements, thus tolerating the uptake of such elements [206].

Among the different functions of biominerals in the plant kingdom [201], detoxification of metals has been reported in different plant species. Several studies demonstrated the role of Ca oxalate crystals in the incorporation of metals [201, 208, 209]. For example, in *Eichhornia crassipes* plants, cultured in jars containing waters with different amounts of Pb and Cd, metal contents in Ca oxalate crystals increased progressively over time of exposure [209]. The presence of Cd in Ca oxalate crystals has been documented also in various tissues of stems of tomato plants [208].

Beside Ca oxalate, there are other biominerals that can contribute to metal detoxification in plants. Metal sequestration with phosphate has been reported in roots and needles of *P. sylvestris*, where pyromorphite ($Pb_5(PO_4)_3(Cl, OH)$) occurs as polycrystalline aggregates in bulges of the cell wall [26], and it was interpreted as a defence mechanism of the plant against Pb pollution. The graminaceous plant *Festuca rubra* (red fescue) precipitates Zn-rich phyllomanganate nanoparticles with constant Zn:Mn and Ca:Mn atomic ratios (0.46 and 0.38, respectively) [207] (Fig. 6e, f). Iron biominerals (mainly jarosite, ferrihydrite, hematite and spinel phases) were found at the cellular level in tissues of roots, stems and leaves of *Imperata cylindrica* from the mine-impacted Rio Tinto river (Iberian Pyritic Belt) [210, 211].

The beneficial role of silica in mitigating various abiotic stresses such as metal toxicity has been recognised by several authors for many instances [187, 201, 212]. Silicon can act through different mechanisms: (i) co-precipitation or complexation of toxic metals with Si, (ii) reducing active heavy metal ions in growth media, (iii) compartmentalization of metals within plants, (iv) reducing metal uptake and translocation, and (v) stimulation of antioxidant systems in plants. Silicon can decrease availability of phytotoxic metals affecting the soil properties [212] such as the pH value and metal speciation by formation of silicate complexes. Reduction of metal uptake and translocation in the presence of Si has been observed for Cd, Cu, Cr and Zn in many plant species such as rice, maize, cotton and wheat, and it can

occur through several processes (e.g., stimulation of root exudates, reduction of the apoplasmic transport of metals, deposition of Si near the endoderm etc.). The effect of Si on metal uptake and translocation varies with plant species [187] (and references therein). Metal toxicity can be reduced also by the co-precipitation of Si with metals as observed by Neumann et al. [213] that reported the precipitation of a Zn-silicate in the epidermal cell walls of *Minuartia verna* ssp. *Hercynica*, and by Neumann and zur Nieden [214] that investigated Zn precipitation as silicate in the cytoplasm of *Cardaminopsis*.

4.5 Critical Zone

The Critical Zone (CZ) is defined as the thin outer skin of Earth's surface ranging from the top of the canopy layer down to the lower limits of groundwater [215]. The term CZ was first coined by the US National Research Council [216] as "… *the heterogeneous, near surface environment in which complex interactions involving rock, soil, water, air and living organisms regulate the natural habitat and determine availability of life sustaining resources*" [217, 218]. These complex biogeochemical-physical processes evolve in response to tectonic, climate, and anthropogenic forcing over vastly different timescales affecting the hydrosphere, lithosphere, pedosphere, atmosphere, and biosphere [215, 218–220]. In the CZ, the pore water can contain metals as free ions or complexed to inorganic or organic ligands, and both are subject mainly to the following processes: (i) diffusion in porous media and transport through the soil profile into groundwater, (ii) uptake by plants, (iii) sorption on mineral surfaces, natural organic matter, and microbes, (iv) precipitation as solid phases [221]. As a response to the variations in these processes, the CZ is characterised by a huge heterogeneity both vertically, recognizable in distinct layers of weathered rock, regolith, and soil (extending from organotrophic in the near surface to oligotrophic conditions at depth), and laterally, due to the diversity of landscapes and the distribution of soils across them [215, 222].

In the root and unsaturated zones, plants and their fungal symbionts physically open the regolith while seeking out water resources and mining for nutrients (e.g., P, K, Ca, Mg etc.) providing physical disturbance at the micro- and macroscales and inducing preferential flow paths. Also, fungal symbionts can increase fractures in regolith by fungal hyphae that are able to exploit microfractures inaccessible to plant roots alone [215]. The vadose zone is subject to fluctuations between wetting and drying conditions. During drying periods, evapotranspiration causes the increase of solute concentrations, leading to precipitation of soluble salts such as sulphates and carbonates. Subsequently, during wetting conditions, these salts are rapidly re-solubilized, and elements are re-mobilised into the pore water [223]. When pores are filled with aqueous solution, weathering reactions are enhanced by the production of organic acids, extracellular enzymes and complexing ligands (e.g. siderophores), pH modification due to CO_2 respiration, mineral mining by roots and fungal hyphae, and by microbial colonization of mineral surfaces (e.g., biotite, Fe oxides, pyrite)

[215]. Bioavailability of inorganic contaminants can change during weathering of primary phases and possible formation of authigenic minerals, depending on mineral transformation rates and the solubility of newly formed secondary minerals [178].

In the unsaturated zone, incongruent weathering of primary to secondary minerals promotes formation of clay-sized layer silicates and different oxides and/or hydroxides of Fe, Al, and Mn. These phases are effective sequestering agents for metals and metalloids (including radionuclides) due to their (i) high specific surface area (10–800 m^2/g), (ii) high surface charge and (iii) reactive surface functional groups [178, 224]. Although the saturated zone is often less altered than the root and unsaturated zones, due to the longer residence times of groundwaters that allow closer approach to equilibrium with soil minerals, (hydr)oxide precipitates can coat primary mineral surfaces, altering their surface reactivity and controlling metal mobility [178, 225]. Secondary clay minerals can interact with natural organic matter (complex mixture of biopolymers such as proteins, carbohydrates, aliphatic biopolymers, lignin), stabilizing it against microbial degradation. The association between minerals and organic compounds affects the behaviour of particle surfaces that can (i) retard the advective–diffusive transport and deposition of solutes and colloidal particles, or (ii) play a relevant role in the nucleation and growth of authigenic precipitates [178]. It is worth noting that the decomposition of natural organic matter by organisms leads to the formation of dissolved organic matter that form stable complexes with metals due to the presence of polar (e.g. carboxyl, hydroxyl) functional groups, potentially increasing pollutant mobility [178].

Davranche et al. [226] (and references therein) highlighted the role of electron transfer in the CZ, due to both biotic and abiotic mechanisms, that controls the fate of inorganic and organic contaminants, whether redox-sensitive or not. Usually, deep horizons and long-term waterlogged systems are characterised by lower amount of dissolved O_2 than upper layers, due to biomass consumption (for respiration), leading to the development of redox gradients. Manganese and Fe-bearing minerals can act as both electron donors and acceptors because Mn and Fe in these phases can have multiple redox states (e.g., magnetite, and green rusts or layered double Fe hydroxides), and they can precipitate or dissolve as a result of redox reactions providing or removing reactive sorption surfaces for chemicals, also they can activate co-precipitation processes. In addition, natural organic matter and microorganisms can promote abiotic electron transfer with mineral surfaces, catalyzing redox reactions (see [226] for a thorough review on natural organic matter and electron transfer).

Microbes, occurring mainly in biofilms spread within soils, actively contribute to the redox gradient of the CZ by forming microenvironments characterised by specific physico-chemical properties (e.g., pH, Eh, etc.). Metabolic processes allow to distinguish prokaryotes in phototrophs (conversion of the light energy into chemical energy when light is available), chemo-organotrophs (oxidation of organic compound), chemo-lithotrophs (oxidation of inorganic compounds, such as H_2, H_2S, NH_4^+, Fe^{2+}, Mn^{2+}, As^{3-}, etc.), anaerobes (anaerobic respiration using Mn^{4+}, Fe^{3+}, SO_4^{2-}, NO_3^-, etc.). Both chemo-lithotrophic and anaerobic microbes can influence the mobility

and toxicity of inorganic pollutants [152, 226, 227]. For example, sulphur/sulphide-oxidizing bacteria cause chemo-lithotrophic leaching of particles, resulting in mobilization of pollutants from soil, while sulphate-reducing bacteria (SRB) can activate the precipitation of stable sulphides, removing chalcophile elements such as Zn, Cd, Cu, Co, Ni etc. [3, 152, 227].

Apart from being important because of their metabolism, microbes can influence metal and/or metalloid speciation, and thus their mobility, in a wide range of processes, including mineral bioweathering and biodeterioration, biosorption processes (e.g. cell wall and other structural biomolecules, metabolites, metal-binding peptides, EPS), intracellular accumulation by transport mechanisms, organellar localization, intracellular sequestration and bioprecipitation, extracellular biomineralization [228].

Several research approaches of varying complexity have been developed to quantify biogeochemical processes in the CZ. The hyporheic zone, the active ecotone between the surface stream and groundwater [229], is an important CZ whose evolution can be investigated by stream solute chemistry. Specifically, the tracer injection technique provides concentration-discharge data, a powerful tool to compare stream behaviour across catchments [230, 231]. In the hyporheic zone, solute release/uptake is ruled by dissolution, precipitation and sorption reaction rates, cation exchange capacity of clays, and biotic processes. In turn, concentration-discharge values in streams are mainly influenced by (i) bedrock lithology, (ii) geomorphic regime, (iii) organic matter and solute source mass distribution, (iv) water residence time, (v) subsurface flow paths, (vi) seasonality and storm events, (vii) cation exchange processes, and (viii) anthropogenic contributions [230, 232]. As a consequence of the balance among processes occurring in the hyporheic zone, this CZ can attenuate or contribute anthropogenic pollutants. Sewage discharges to surface waters can significantly increase pore water nutrient contents, altering hyporheic biogeochemical processes. Chemicals in agricultural runoff or contaminants from polluted areas can move from surface water into groundwater with little change in concentration or can be degraded and/or stabilised within the hyporheic zone. Also, metals and other pollutants can move from groundwater into surface water through the hyporheic interface [229].

The CZ can be considered as a biogeochemical reactor, open to fluxes of matter (gas, liquid and solid form) and energy (heat and reduced carbon compounds fixed through photosynthesis) and plays an essential role in natural and managed ecosystems. Indeed biogeochemical processes occurring at the atomic scale influence macroscopic to global scale processes [219, 222, 223]. The presence of several exposed solid surfaces (e.g., minerals, plants, microorganisms) affects transport, retention (i.e. sorption), and chemical transformation of solutes. At the nano and microscale, biogeochemical reactions drive the evolution of particle surfaces and their reactivity, whereas at the watershed scale, they control stream and groundwater quality [178].

5 Biomineral Processes and Sustainability

In this section we focus on the relevance of biomineral processes to the environment and environmental management. For this purpose, we present some examples of application of biomineral science to environmental management.

5.1 Biometallurgy and Circular Economy

Through geological time, microorganisms developed their capability to work as expert biometallurgists in many different microenvironments. To date, biometallurgy techniques are applied globally to recover Cu and many other metals [233, 234] (and references therein). As shown in Table 1, microorganisms are pioneers also in extreme environments and have the potential to extract or precipitate metals relevant to both industrial and environmental processes [235, 236]. For this reason, bacteria and fungi are used in the mining industry to increase recovery rates and offer unique tools for sustainable mining and reuse of large volumes of mine waste produced in the past activity.

Pyrite is the most common sulphur-bearing mineral in the Earth's crust, and ^{32}S enrichment in pyrite mineralisation driven by sulphate reducing microbes clearly provides evidence in the geological record [237]. Ohmoto and Lasaga [238] first pointed out that the rates of sulphate reduction by non-bacterial processes involving a variety of reductants are also dependent on T, pH, activities of S species in solution and appear to be fast enough to become geochemically important only at temperatures above about 200 °C. The process of sulphate reduction implies the transfer of eight electrons, is endothermic and is not likely to occur in nature at ambient temperature without microbial activity [239]. Sulphate reducing bacteria (SRB) play a key role in surface environments. SRB are part of the organism's microbiome and are ubiquitous in the environment. Framboidal morphology of minerals such as pyrite, greigite, magnetite, magnesioferrite, marcasite, as well of supposedly secondary minerals such as hematite, limonite, chalcocite, chalcopyrite, bornite, sphalerite, galena are known from the Archean [240, 241] and are often indicative of BIM. Though framboidal iron sulphides are ubiquitous in near-surface environments, SRB play a pivotal role in biomineral formation as they increase sulphide concentrations in water, and then induce formation of framboidal metal sulphides. Recently, zinc sulphide forming in SRB natural biofilms have been observed by mineralogists and environmental scientists [242].

Most often, biometallurgy involves heap leaching with use of non-autochthonous microbial strains that are commercially available. The challenge is now to use biometallurgy techniques to apply circular economy paradigm for many critical metals such as Sb, REE, Co, Ni and so on [243]. Staicu et al. [244] isolated *Bacillus sp. Abq*, belonging to *Bacillus cereus* sensu lato, finding its unusual property of precipitating Pb(II) by using cysteine, which is degraded intracellularly to produce hydrogen

sulfide (H_2S). H_2S is then exported to the extracellular environment to react with Pb(II), yielding PbS (galena). Paganin et al. [245] investigated microbial diversity in core samples from different areas of the same abandoned mine district and obtained different inocula (Fig. 7a, b). Moreover, they were able to reprecipitate ZnS by using the selected inocula (Fig. 7c, d) from the mine polluted water with removal rates up to 100%. Summarizing, we are now accumulating a large body of knowledge that can be transferred soon to industrial scale applications that pave the way to sustainable technologies for recovering metals from wastes.

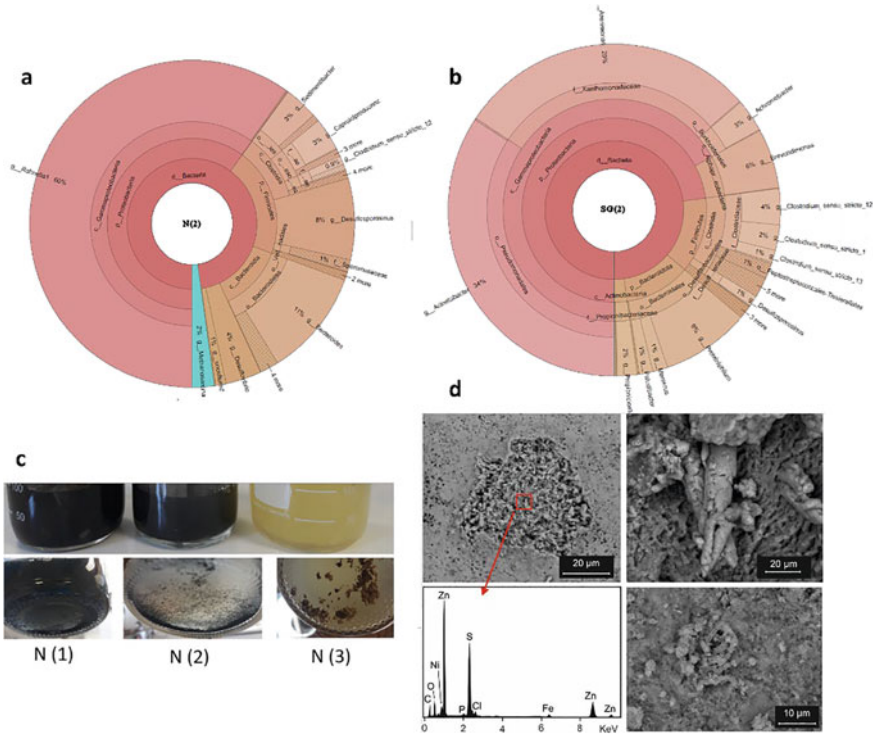

Fig. 7 **a** and **b** Krona plot at the genus level for two different areas indicating their microbial biodiversity; **a** inoculum N_2 cultured from the Naracauli mine area microbial community; **b** inoculum SG(2) cultured from the San Giorgio valley mine area microbial community; **c** growth of sulphate-reducing bacteria in the three different media inoculated with sediments of Rio Naracauli and details of Fe sulfide (black) and Zn sulfide (brownish) precipitates; **d** SEM–EDS analysis: BSE images of the bioprecipitates recovered from experiments performed with inoculum cultured from Rio Naracauli core sediments and mine polluted waters. Images from Paganin et al. [245], Copyright (2018) Paganin et al., under the Creative Commons Attribution License

5.2 Secondary Ores and Environmental Resilience

There is a growing body of literature that points out the interplay among biological activity and the response of environment to stress, also on a time scale of a few years. Figures 2g, 7a, b provide discrete evidence of the microbial biodiversity over a short spatial distance. Moreover, our research group found that cyanobacterial biofilm can lead to huge seasonal and spatial variability in biomineralization processes along the same riverbed without any apparent change in the geochemical properties of the investigated systems [30, 92, 93, 246].

Dore et al. [3] analysed biomineralization processes and the environmental status in four riverbeds affected by historical mine pollution. Growth of dense vegetation in a riverbed has a primary effect of favouring the sedimentation of fine sediments, and a secondary effect of favouring biogeochemical processes in the hyporheic zone, which is part of CZ. In fact, when the erosional regime is changed to a sedimentation regime due to the slow velocity of water retained from the stems like in a wetland-like system, many different biomineralization processes can become effective in trapping metals in the sediments that constitute the hyporheic zone of the riverbed. De Giudici et al. [247] and Dore et al. [3] show that the natural process of vegetation growth in historical-mine-activity-degraded riverbeds serves as an example for the development of effective industrial-scale biogeochemical processes previously described in the literature by, for instance, Labrenz et al. [242]. In the case of Rio San Giorgio in southwestern Sardinia, trapping of fine sediments within the stems of *Phragmites australis* and the riverbed allows the dominance of SRB communities, leading to the formation of abundant biogenically induced base metal sulphides. Plant roots also favour the formation of biominerals such as hemimorphite and hydrozincite, thus contributing to natural abatement of Zn and other metals. Notably, these sediments can be considered themselves as future secondary ores to be exploited with a new generation of biometallurgy techniques.

6 Remarks and Conclusion

In this chapter we summarized the impact of biomineralization on both Earth and environmental processes. Through the whole geological record, the co-evolution of life and minerals led to a significant diversity of biominerals, of which more than 160 are known today. About 120 biominerals are organic compounds, phosphates, carbonates, hydroxides, and oxides. This is partially related to the chemical composition of DNA and RNA and organic molecules in general, that are made of C, H, O, N and P. Diversity of biomineralization processes increased with evolution of life, and biominerals are made to assure many different physiological purposes such as detoxification. Actually, biominerals cover almost all the mineral classes comprising silicates, and biomineral processes involve toxic elements such as Pb and As.

Biomineralization processes co-exerted a profound impact on Earth by altering the composition of water, atmosphere, and soil. We stressed that biomineralization processes can have a profound impact on environmental systems even on short time scales (few years). Understanding the environment where biomineralization occur, such as biofilm and other water soil microenvironments, is then central to the understanding the biomineralization impact on our environment. In turn this shed light on the impact of biomineralization processes on sustainability and related technologies. As an example, we mentioned the role of authigenic minerals in the critical zone controlling mobility of metals.

As final remarks for the (bio)mineralogist, it is worth noting that biomineral studies are intrinsically interdisciplinary. The capacity building that the scientific community can develop in the area of mineral-biosphere interactions is proportional to our capability of selecting (micro)organisms able to build a specific microenvironment and to our skills in reproducing their biomineral processes. It should also be noted that the capability to reproduce biomineralization driven by microorganisms in industrial processes non in vivo industrial processes is still a visionary approach, that can reveal new and highly sustainable processes in future. Finally, characterization of crystal and mineral structure down to the nanoscale is central to understanding biominerals. Biominerals are often poorly crystalline, small, and dispersed in complex matrices. Their recognition and understanding of their role often need the use of advanced and multiscale/multiphysics approaches combining complementary techniques.

Acknowledgements We thank P. Lattanzi and R. B Wanty for their suggestions and comments on a preliminary version of this manuscript.

References

1. Van Cappellen P (2003) Biomineralization and global biogeochemical cycles. Rev Mineral Geochem 54:357–381. https://doi.org/10.2113/0540357
2. Trembath-Reichert E, Wilson JP, McGlynn SE, Fischer WW (2015) Four hundred million years of silica biomineralization in land plants. Proc Natl Acad Sci U S A 112:5449–5454. https://doi.org/10.1073/pnas.1500289112
3. Dore E, Fancello D, Rigonat N et al (2020) Natural attenuation can lead to environmental resilience in mine environment. Appl Geochem. https://doi.org/10.1016/j.apgeochem.2020.104597
4. Birarda G, Buosi C, Caridi F et al (2021) Plastics, (bio)polymers and their apparent biogeochemical cycle: an infrared spectroscopy study on foraminifera. Environ Pollut 279:116912. https://doi.org/10.1016/j.envpol.2021.116912
5. Fitzer SC, McGill RAR, Torres Gabarda S et al (2019) Selectively bred oysters can alter their biomineralization pathways, promoting resilience to environmental acidification. Glob Chang Biol 25:4105–4115. https://doi.org/10.1111/gcb.14818
6. Caraballo MA, Asta MP, Perez JPH, Hochella MF (2021) Past, present and future global influence and technological applications of iron-bearing metastable nanominerals. Gondwana Res. https://doi.org/10.1016/j.gr.2021.11.009
7. Lowenstam HA (1981) Minerals formed by organisms. Science 211(80):1126–1131

8. Skinner HCW (2005) Biominerals. Mineral Mag 69:621–641. https://doi.org/10.1180/0026461056950275
9. Strunz H (1941) Mineralogische tabellen : im Auftrage der Deutschen Mineralogischen Gesellschaft/herausgegeben von Hugo Strunz. Becker & Erler
10. Lowenstam H (1974) Impact of life on chemical and physical processes. In: Goldberg ED (ed) The sea, marine chemistry. John Wiley and Sons, New York, pp 715–796
11. Lowenstam HA, Weiner S (1983) Mineralization by organisms and the evolution of biomineralization. In: Westbroek P, de Jong EW (eds) Biomineralization and biological metal accumulation. Springer, Netherlands, Dordrecht, pp 191–203
12. Weiner S, Dove PM (2003) An overview of biomineralization processes and the problem of the vital effect. Rev Mineral Geochem 54:1–29. https://doi.org/10.2113/0540001
13. Hazen RM, Papineau D, Bleeker W et al (2008) Mineral evolution. Am Mineral 93:1693–1720. https://doi.org/10.2138/am.2008.2955
14. Podda F, Zuddas P, Minacci A et al (2000) Heavy metal coprecipitation with hydrozincite [$Zn_5(CO_3)_2(OH)_6$] from mine waters caused by photosynthetic microorganisms. Appl Environ Microbiol 66:5092–5098
15. Wilkin RT, Barnes HL (1996) Pyrite formation by reactions of iron monosulfides with dissolved inorganic and organic sulfur species. Geochim Cosmochim Acta 60:4167–4179. https://doi.org/10.1016/S0016-7037(97)81466-4
16. Tazaki K, Rafiqul IA, Nagai K, Kurihara T (2003) $FeAs_2$ biomineralization on encrusted bacteria in hot springs: an ecological role of symbiotic bacteria. Can J Earth Sci 40:1725–1738. https://doi.org/10.1139/e03-081
17. Ferris FG, Fyfe WS, Beveridge TJ (1987) Bacteria as nucleation sites for authigenic minerals in a metal-contaminated lake sediment. Chem Geol 63:225–232. https://doi.org/10.1016/0009-2541(87)90165-3
18. International Mineralogical Association (2021) IMA database of mineral properties. https://rruff.info/ima/. Accessed 18 Nov 2021
19. Lowenstam HA, Weiner S (1989) On biomineralization. Oxford University Press, New York
20. Morin G, Juillot F, Casiot C et al (2003) Bacterial formation of tooeleite and mixed Arsenic(III) or Arsenic(V)—Iron(III) gels in the carnoulès acid mine drainage, France. A XANES, XRD, and SEM study. Environ Sci Technol 37:1705–1712. https://doi.org/10.1021/es025688p
21. Power IM, Wilson SA, Thom JM et al (2007) Biologically induced mineralization of dypingite by cyanobacteria from an alkaline wetland near Atlin, British Columbia, Canada. Geochem Trans 8:1–16. https://doi.org/10.1186/1467-4866-8-13
22. Schultze-Lam S, Beveridge TJ (1994) Nucleation of celestite and strontianite on a cyanobacterial S-layer. Appl Environ Microbiol 60:447–453. https://doi.org/10.1128/aem.60.2.447-453.1994
23. Dogan AU, Dogan M, Chan DCN, Wurster DE (2005) Bassanite from Salvadora persica: a new evaporitic biomineral. Carbonates Evaporites 20:2–7. https://doi.org/10.1007/BF03175444
24. Frankel RB, Bazylinski DA (2003) Biologically induced mineralization by bacteria. Rev Mineral Geochem 54:95–114. https://doi.org/10.2113/0540095
25. Zachara JM, Kukkadapu RK, James K et al (2002) Biomineralization of poorly crystalline Fe(III) oxides by dissimilatory metal reducing bacteria (DMRB) biomineralization of poorly crystalline Fe(III) oxides by dissimilatory metal reducing bacteria (DMRB). Geomicrobiol J 37–41
26. Bizo ML, Nietzsche S, Mansfeld U et al (2017) Response to lead pollution: mycorrhizal *Pinus sylvestris* forms the biomineral pyromorphite in roots and needles. Environ Sci Pollut Res 24:14455–14462. https://doi.org/10.1007/s11356-017-9020-7
27. Konhauser KO, Fyfe WS, Schultze-Lam S et al (1994) Iron phosphate precipitation by epilithic microbial biofilms in Arctic Canada. Can J Earth Sci 31:1320–1324. https://doi.org/10.1139/e94-114
28. Akai J, Akai K, Ito M et al (1999) Biologically induced iron ore at Gunma iron mine, Japan. Am Mineral 84:171–182. https://doi.org/10.2138/am-1999-1-219

29. Gadd GM, Rhee YJ, Stephenson K, Wei Z (2012) Geomycology: metals, actinides and biominerals. Environ Microbiol Rep 4:270–296. https://doi.org/10.1111/j.1758-2229.2011.00283.x
30. Podda F, Medas D, De Giudici G et al (2014) Zn biomineralization processes and microbial biofilm in a metal-rich stream (Naracauli, Sardinia). Environ Sci Pollut Res. https://doi.org/10.1007/s11356-013-1987-0
31. Medas D, Lattanzi P, Podda F et al (2014) The amorphous Zn biomineralization at Naracauli stream, Sardinia: electron microscopy and X-ray absorption spectroscopy. Environ Sci Pollut Res 21:6775–6782. https://doi.org/10.1007/s11356-013-1886-4
32. Gorbushina AA, Boettcher M, Brumsack HJ et al (2001) Biogenic forsterite and opal as a product of biodeterioration and lichen stromatolite formation in table mountain systems (Tepuis) of Venezuela. Geomicrobiol J 18:117–132. https://doi.org/10.1080/01490450151079851
33. Konhauser KO (1997) Bacterial iron biomineralisation in nature. FEMS Microbiol Rev 20:315–326. https://doi.org/10.1016/S0168-6445(97)00014-4
34. Zeyen N, Benzerara K, Li J et al (2015) Formation of low-T hydrated silicates in modern microbialites from Mexico and implications for microbial fossilization. Front Earth Sci 3:1–23. https://doi.org/10.3389/feart.2015.00064
35. Konhauser KO, Fyfe WS, Ferris FG, Beveridge TJ (1993) Metal sorption and mineral precipitation by bacteria in two Amazonian river systems: Rio Solimoes and Rio Negro, Brazil. Geology 21:1103–1106. https://doi.org/10.1130/0091-7613(1993)021%3c1103:MSAMPB%3e2.3.CO;2
36. Ta K, Peng X, Chen S et al (2017) Hydrothermal nontronite formation associated with microbes from low-temperature diffuse hydrothermal vents at the South Mid-Atlantic Ridge. J Geophys Res Biogeosciences 122:2375–2392. https://doi.org/10.1002/2017JG003852
37. Burne RV, Moore LS, Christy AG et al (2014) Stevensite in the modern thrombolites of Lake Clifton, Western Australia: a missing link in microbialite mineralization? Geology 42:575–578. https://doi.org/10.1130/G35484.1
38. Burford EP, Kierans M, Gadd GM (2003) Geomycology: fungi in mineral substrata. Mycologist 17:98–107. https://doi.org/10.1017/S0269915X03003112
39. Bazylinski D, Frankel R (2003) Biologically controlled mineralization in prokaryotes. Rev Mineral Geochem 54:217–247. https://doi.org/10.2113/0540217
40. De Giudici G, Medas D, Cidu R et al (2017) Application of hydrologic-tracer techniques to the Casargiu adit and Rio Irvi (SW-Sardinia, Italy): Using enhanced natural attenuation to reduce extreme metal loads. Appl Geochem 96:42–54. https://doi.org/10.1016/j.apgeochem.2018.06.004
41. Frau F, Medas D, Da Pelo S et al (2015) Environmental effects on the aquatic system and metal discharge to the mediterranean sea from a near-neutral zinc-ferrous sulfate mine drainage. Water Air Soil Pollut 226:226–255. https://doi.org/10.1007/s11270-015-2339-0
42. Chasteen ND, Harrison PM (1999) Mineralization in ferritin: an efficient means of iron storage. J Struct Biol 126:182–194. https://doi.org/10.1006/jsbi.1999.4118
43. Woo KM, Jun J-H, Chen VJ et al (2007) Nano-fibrous scaffolding promotes osteoblast differentiation and biomineralization. Biomaterials 28:335–343. https://doi.org/10.1016/j.biomaterials.2006.06.013
44. Boraldi F, Burns JS, Bartolomeo A et al (2018) Mineralization by mesenchymal stromal cells is variously modulated depending on commercial platelet lysate preparations. Cytotherapy 20:335–342. https://doi.org/10.1016/j.jcyt.2017.11.011
45. Rui Y, Qian C (2021) The regulation mechanism of bacteria on the properties of biominerals. J Cryst Growth 570:126214. https://doi.org/10.1016/j.jcrysgro.2021.126214
46. Bernal JD (1951) The physical basis of life. Routledge and Paul, London
47. Hazen RM (2006) Mineral surfaces and the prebiotic selection and organization of biomolecules. Am Mineral 91:1715–1729. https://doi.org/10.2138/am.2006.2289
48. Antonietti M, Förster S (2003) Vesicles and liposomes: a self-assembly principle beyond lipids. Adv Mater 15:1323–1333. https://doi.org/10.1002/adma.200300010

49. Hazen R (2004) Chiral crystal faces of common rock-forming minerals. In: Palyi G, Zucchi C, Caglioti L (eds) Progress in biological chirality. Elsevier, Oxford UK, pp 137–151
50. Downs RT, Hazen RM (2004) Chiral indices of crystalline surfaces as a measure of enantioselective potential. J Mol Catal A-Chem 216:273–285. https://doi.org/10.1016/J.MOLCATA.2004.03.026
51. Orme CA, Noy A, Wierzbicki A et al (2001) Formation of chiral morphologies through selective binding of amino acids to calcite surface steps. Nature 411:775–779. https://doi.org/10.1038/35081034
52. Hazen RM, Sholl DS (2003) Chiral selection on inorganic crystalline surfaces. Nat Mater 2:367–374. https://doi.org/10.1038/nmat879
53. De Yoreo JJ, Dove PM (2004) Shaping crystals with biomolecules. Science 306(80):1301–1302. https://doi.org/10.1126/science.1100889
54. Bally AW, Palmer AR (1989) The geology of North America—an overview
55. Sumner DY (1997) Carbonate precipitation and oxygen stratification in late Archean seawater as deduced from facies and stratigraphy of the Gamohaan and Frisco formations, Transvaal Supergroup, South Africa. Am J Sci 297:455 LP–487. https://doi.org/10.2475/ajs.297.5.455
56. Carter PW, Mitterer RM (1978) Amino acid composition of organic matter associated with carbonate and non-carbonate sediments. Geochim Cosmochim Acta 42:1231–1238. https://doi.org/10.1016/0016-7037(78)90116-3
57. Weiner S, Addadi L (1997) Design strategies in mineralized biological materials. J Mater Chem 7:689–702. https://doi.org/10.1039/A604512J
58. Aizenberg J, Tkachenko A, Weiner S et al (2001) Calcitic microlenses as part of the photoreceptor system in brittlestars. Nature 412:819–822. https://doi.org/10.1038/35090573
59. Teng HH, Dove PM (1997) Surface site-specific interactions of aspartate with calcite during dissolution; implications for biomineralization. Am Mineral 82:878–887. https://doi.org/10.2138/am-1997-9-1005
60. Teng HH, Dove PM, Orme CA, De Yoreo JJ (1998) Thermodynamics of calcite growth: baseline for understanding biomineral formation. Science 282(80):724–727. https://doi.org/10.1126/science.282.5389.724
61. Teng HH, Dove P, Yoreo J (2000) Kinetics of calcite growth: surface processes and relationships to macroscopic rate laws. Geochim Cosmochim Acta 64:2255–2266. https://doi.org/10.1016/S0016-7037(00)00341-0
62. Dana ED (1958) A textbook of mineralogy, 4th Editio. John Wiley and Sons, New York
63. Hazen RM, Filley TR, Goodfriend GA (2001) Selective adsorption of l- and d-amino acids on calcite: Implications for biochemical homochirality. Proc Natl Acad Sci 98:5487 LP–5490. https://doi.org/10.1073/pnas.101085998
64. Lahav N, White D, Chang S (1978) Peptide formation in the prebiotic era: thermal condensation of glycine in fluctuating clay environments. Science 201(80):67–69. https://doi.org/10.1126/science.663639
65. Ferris JP (1993) Catalysis and prebiotic RNA synthesis. Orig life Evol Biosph 23:307–315. https://doi.org/10.1007/BF01582081
66. Ferris JP (1999) Prebiotic synthesis on minerals: bridging the prebiotic and RNA worlds. Biol Bull 196:311–314. https://doi.org/10.2307/1542957
67. Ferris JP (2005) Mineral catalysis and prebiotic synthesis: montmorillonite-catalyzed formation of RNA. Elements 1:145–149. https://doi.org/10.2113/gselements.1.3.145
68. Holm NG, Ertem G, Ferris JP (1993) The binding and reactions of nucleotides and polynucleotides on iron oxide hydroxide polymorphs. Orig life Evol Biosph J Int Soc Study Orig Life 23:195–215. https://doi.org/10.1007/BF01581839
69. Ferris JP, Ertem G (1992) Oligomerization of ribonucleotides on montmorillonite: reaction of the 5′-phosphorimidazolide of adenosine. Science 257(80):1387–1389. https://doi.org/10.1126/science.1529338
70. Ferris JP, Ertem G (1993) Montmorillonite catalysis of RNA oligomer formation in aqueous solution. A model for the prebiotic formation of RNA. J Am Chem Soc 115:12270–12275. https://doi.org/10.1021/ja00079a006

71. Ertem G, Ferris JP (1996) Synthesis of RNA oligomers on heterogeneous templates. Nature 379:238–240. https://doi.org/10.1038/379238a0
72. Ertem G, Ferris JP (1997) Template-directed synthesis using the heterogeneous templates produced by montmorillonite catalysis. A possible bridge between the prebiotic and RNA worlds. J Am Chem Soc 119:7197–7201. https://doi.org/10.1021/ja970422h
73. Zheng J, Li Z, Wu A, Zhou H (2003) AFM studies of DNA structures on mica in the presence of alkaline earth metal ions. Biophys Chem 104:37–43. https://doi.org/10.1016/s0301-4622(02)00335-6
74. Cervantes NAG, Gutiérrez-Medina B (2014) Robust deposition of lambda DNA on mica for imaging by AFM in air. Scanning 36:561–569. https://doi.org/10.1002/sca.21155
75. Thomson NH, Kasas S, Smith et al (1996) Reversible binding of DNA to mica for AFM imaging. Langmuir 12:5905–5908. https://doi.org/10.1021/la960497j
76. Valdrè G, Moro D, Ulian G (2011) Nucleotides, RNA and DNA selective adsorption on atomic-flat Mg–Al-hydroxysilicate substrates. Micro Nano Lett 6:922–926(4). https://doi.org/10.1049/mnl.2011.0546
77. Moro D, Ulian G, Valdrè G (2020) Nano-atomic scale hydrophobic/philic confinement of peptides on mineral surfaces by cross-correlated SPM and quantum mechanical DFT analysis. J Microsc 280:204–221. https://doi.org/10.1111/jmi.12923
78. Meldrum FC, Cölfen H (2008) Controlling mineral morphologies and structures in biological and synthetic systems. Chem Rev 108:4332–4432. https://doi.org/10.1021/cr8002856
79. Bonn M, Bakker HJ, Tong Y, Backus EHG (2012) No ice-like water at aqueous biological interfaces. Biointerphases 7:20. https://doi.org/10.1007/s13758-012-0020-3
80. Singer SJ, Nicolson GL (1972) The fluid mosaic model of the structure of cell membranes. Science 175:720–731. https://doi.org/10.1126/science.175.4023.720
81. Steed JW, Atwood JL (2009) Supramolecular chemistry, 2nd edn. Wiley, Chichester
82. Lehn J-M (1988) Supramolecular chemistry—scope and perspectives molecules, supermolecules, and molecular devices (nobel lecture). Angew Chemie Int Ed English 27:89–112. https://doi.org/10.1002/anie.198800891
83. Lehn JM (1988) Supramolekulare Chemie – Moleküle, Übermoleküle und molekulare Funktionseinheiten (Nobel-Vortrag). Angew Chemie 100:91–116. https://doi.org/10.1002/ANGE.19881000110
84. Breslow R (2005) Artificial enzymes. Wiley-VCH, Weinheim
85. Pedersen C (1988) The discovery of crown ethers (noble lecture). Angew Chemie Int Ed English 27:1021–1027. https://doi.org/10.1002/anie.198810211
86. Pedersen CJ (1988) Die Entdeckung der Kronenether (Nobel-Vortrag). Angew Chemie 100:1053–1059. https://doi.org/10.1002/ange.19881000805
87. Breuer M, Rosso KM, Blumberger J (2014) Electron flow in multiheme bacterial cytochromes is a balancing act between heme electronic interaction and redox potentials. Proc Natl Acad Sci U S A 111:611–616. https://doi.org/10.1073/pnas.1316156111
88. Sand KK, Rodriguez-Blanco JD, Makovicky E et al (2012) Crystallization of $CaCO_3$ in water-alcohol mixtures: spherulitic growth, polymorph stabilization, and morphology change. Cryst Growth Des 12:842–853. https://doi.org/10.1021/cg2012342
89. Penn RL, Banfield JF (1998) Oriented attachment and growth, twinning, polytypism, and formation of metastable phases; insights from nanocrystalline TiO_2. Am Mineral 83:1077–1082. https://doi.org/10.2138/am-1998-9-1016
90. Banfield JF, Welch SA, Zhang H, et al (2000) Aggregation-based crystal growth and microstructure development in natural iron oxyhydroxide biomineralization products. Science 289(80):751–754. https://doi.org/10.1126/science.289.5480.751
91. De Yoreo JJ, Gilbert PUPA, Sommerdijk NAJM, et al (2015) Crystal growth. Crystallization by particle attachment in synthetic, biogenic, and geologic environments. Science 349(80):aaa6760. https://doi.org/10.1126/science.aaa6760
92. Medas D, De Giudici G, Podda F et al (2014) Apparent energy of hydrated biomineral surface and apparent solubility constant: an investigation of hydrozincite. Geochim Cosmochim Acta. https://doi.org/10.1016/j.gca.2014.05.019

93. De Giudici G, Podda F, Sanna R et al (2009) Structural properties of biologically controlled hydrozincite: an HRTEM and NMR spectroscopic study. Am Mineral 94:1698–1706. https://doi.org/10.2138/am.2009.3181
94. Beniash E, Aizenberg J, Addadi L, Weiner S (1997) Amorphous calcium carbonate transforms into calcite during sea urchin larval spicule growth. Proc R Soc London Ser B Biol Sci 264:461–465. https://doi.org/10.1098/rspb.1997.0066
95. Politi Y, Arad T, Klein E, et al (2004) Sea urchin spine calcite forms via a transient amorphous calcium carbonate phase. Science 306(80):1161–1164. https://doi.org/10.1126/science.1102289
96. Albéric M, Stifler CA, Zou Z et al (2019) Growth and regrowth of adult sea urchin spines involve hydrated and anhydrous amorphous calcium carbonate precursors. J Struct Biol X 1:100004. https://doi.org/10.1016/j.yjsbx.2019.100004
97. Killian CE, Metzler RA, Gong Y, et al (2011) Self-sharpening mechanism of the sea urchin tooth. Adv Funct Mater 21:682–690. https://doi.org/10.1002/adfm.201001546
98. Weiss IM, Tuross N, Addadi L, Weiner S (2002) Mollusc larval shell formation: amorphous calcium carbonate is a precursor phase for aragonite. J Exp Zool 293:478–491. https://doi.org/10.1002/jez.90004
99. DeVol RT, Sun C-Y, Marcus MA et al (2015) Nanoscale transforming mineral phases in fresh nacre. J Am Chem Soc 137:13325–13333. https://doi.org/10.1021/jacs.5b07931
100. Mahamid J, Sharir A, Addadi L, Weiner S (2008) Amorphous calcium phosphate is a major component of the forming fin bones of zebrafish: indications for an amorphous precursor phase. Proc Natl Acad Sci 105:12748 LP–12753. https://doi.org/10.1073/pnas.0803354105
101. Beniash E, Metzler RA, Lam RSK, Gilbert PUPA (2009) Transient amorphous calcium phosphate in forming enamel. J Struct Biol 166:133–143. https://doi.org/10.1016/j.jsb.2009.02.001
102. Mass T, Giuffre AJ, Sun C-Y, et al (2017) Amorphous calcium carbonate particles form coral skeletons. Proc Natl Acad Sci 114:E7670 LP-E7678. https://doi.org/10.1073/pnas.1707890114
103. Hazen RM, Ferry JM (2010) Mineral evolution: mineralogy in the fourth dimension. Elements 6:9–12. https://doi.org/10.2113/gselements.6.1.9
104. Zhu T, Dittrich M (2016) Carbonate precipitation through microbial activities in natural environment, and their potential in biotechnology: a review. Front Bioeng Biotechnol 4:4. https://doi.org/10.3389/fbioe.2016.00004
105. Schopf JW, Kudryavtsev AB, Czaja AD, Tripathi AB (2007) Evidence of Archean life: stromatolites and microfossils. Precambrian Res 158:141–155. https://doi.org/10.1016/j.precamres.2007.04.009
106. Gong YUT, Killian CE, Olson IC et al (2012) Phase transitions in biogenic amorphous calcium carbonate. Proc Natl Acad Sci 109:6088 LP–6093. https://doi.org/10.1073/pnas.1118085109
107. Boettiger A, Ermentrout B, Oster G (2009) The neural origins of shell structure and pattern in aquatic mollusks. Proc Natl Acad Sci 106:6837 LP–6842. https://doi.org/10.1073/pnas.0810311106
108. Lim KK, Rossbach S, Geraldi NR, et al (2020) The small giant clam, tridacna maxima exhibits minimal population genetic structure in the red sea and genetic differentiation from the Gulf of Aden. Front Mar Sci. https://doi.org/10.3389/fmars.2020.570361
109. Lesser MP (2004) Experimental biology of coral reef ecosystems. J Exp Mar Bio Ecol 300:217–252. https://doi.org/10.1016/j.jembe.2003.12.027
110. Triantaphyllou MV, Baumann K-H, Karatsolis B-T et al (2018) Coccolithophore community response along a natural CO_2 gradient off Methana (SW Saronikos Gulf, Greece, NE Mediterranean). PLoS ONE 13:e0200012. https://doi.org/10.1371/journal.pone.0200012
111. LeKieffre C, Bernhard JM, Mabilleau G, et al (2018) An overview of cellular ultrastructure in benthic foraminifera: new observations of rotalid species in the context of existing literature. Mar Micropaleontol 138:12–32. https://doi.org/10.1016/j.marmicro.2017.10.005
112. Du X, Fan G, Jiao Y et al (2017) The pearl oyster *Pinctada fucata martensii* genome and multi-omic analyses provide insights into biomineralization. Gigascience 6:gix059. https://doi.org/10.1093/gigascience/gix059

113. Rivadeneyra A, Gonzalez-Martinez A, Portela GR et al (2017) Biomineralisation of carbonate and sulphate by the halophilic bacterium Halomonas maura at different manganese concentrations. Extremophiles 21:1049–1056. https://doi.org/10.1007/s00792-017-0965-8
114. Medas D, De Giudici G, Podda F et al (2014) Apparent energy of hydrated biomineral surface and apparent solubility constant: an investigation of hydrozincite. Geochim Cosmochim Acta 140:349–364. https://doi.org/10.1016/j.gca.2014.05.019
115. Roh Y, Zhang C, Vali H et al (2003) Biogeochemical and environmental factors in Fe biomineralization: magnetite and siderite formation. Clays Clay Miner 51:83–95. https://doi.org/10.1346/CCMN.2003.510110
116. Combes C, Cazalbou S, Rey C (2016) Apatite biominerals. Miner 6
117. Beniash E (2011) Biominerals—hierarchical nanocomposites: the example of bone. Wiley Interdiscip Rev Nanomed Nanobiotechnol 3:47–69. https://doi.org/10.1002/wnan.105
118. Vallet-Regí M, Arcos Navarrete D (2016) Biological apatites in bone and teeth. In: nanoceramics in clinical use: from materials to applications (2). The Royal Society of Chemistry, pp 1–29
119. Frankel RB (1991) Iron biominerals: an overview. In: Blakemore R, Frankel R (eds) Iron biominerals. Springer, Boston, pp 1–6
120. Fleming EJ, Cetinić I, Chan CS et al (2014) Ecological succession among iron-oxidizing bacteria. ISME J 8:804–815. https://doi.org/10.1038/ismej.2013.197
121. Richard B (1975) Magnetotactic bacteria. Science 190(80):377–379. https://doi.org/10.1126/science.170679
122. Kaas P, Jones AM (1998) Class polyplacophora: morphology and physiology. In: Beesley PL, Ross GJB, Wells A (eds) Mollusca: the southern synthesis part A, Fauna of Australia. CSIRO, Melbourne, pp 163–174
123. Brooker L, Shaw J (2012) The Chiton Radula: a unique model for biomineralization studies. In: Seto J (ed) Advanced topics in biomineralization. pp 65–84
124. Kisailus D, Nemoto M (2018) Structural and proteomic analyses of iron oxide biomineralization in chiton teeth. In: Matsunaga T, Tanaka T, Kisailus D (eds) Biological magnetic materials and applications. Springer Singapore, Singapore, pp 53–73
125. Moura HM, Unterlass MM (2020) Biogenic metal oxides. Biomimetics (Basel, Switzerland) 5:29. https://doi.org/10.3390/biomimetics5020029
126. Wealthall RJ, Brooker LR, Macey DJ, Griffin BJ (2005) Fine structure of the mineralized teeth of the chiton *Acanthopleura echinata* (Mollusca: Polyplacophora). J Morphol 265:165–175. https://doi.org/10.1002/jmor.10348
127. Weaver JC, Wang Q, Miserez A et al (2010) Analysis of an ultra hard magnetic biomineral in chiton radular teeth. Mater Today 13:42–52. https://doi.org/10.1016/S1369-7021(10)70016-X
128. Ansari MI, Schiwon K, Malik A, Grohmann E (2012) Biofilm formation by environmental bacteria. In: Malik A, Grohmann E (eds) Environmental protection strategies for sustainable development. Strategies for sustainability. Springer, Dordrecht, pp 341–378
129. Karatan E, Watnick P (2009) Signals, regulatory networks, and materials that build and break bacterial biofilms. Microbiol Mol Biol Rev 73:310–347. https://doi.org/10.1128/mmbr.00041-08
130. Awramik SM, Schopf JW, Walter MR (1983) Filamentous fossil bacteria from the Archean of Western Australia. Precambrian Res 20:357–374. https://doi.org/10.1016/0301-9268(83)90081-5
131. Flemming HC (1993) Biofilms and environmental protection. Water Sci Technol 27:1–10. https://doi.org/10.2166/wst.1993.0528
132. Singh R, Paul D, Jain RK (2006) Biofilms: implications in bioremediation. Trends Microbiol 14:389–397. https://doi.org/10.1016/j.tim.2006.07.001
133. Simões M, Simões LC, Vieira MJ (2010) A review of current and emergent biofilm control strategies. LWT - Food Sci Technol 43:573–583. https://doi.org/10.1016/j.lwt.2009.12.008
134. Yin W, Wang Y, Liu L, He J (2019) Biofilms: the microbial "protective clothing" in extreme environments. Int J Mol Sci 20:3423. https://doi.org/10.3390/ijms20143423

135. O'Toole G, Kaplan HB, Kolter R (2000) Biofilm formation as microbial development. Annu Rev Microbiol 54:49–79
136. Hall-Stoodley L, Stoodley P (2002) Developmental regulation of microbial biofilms. Curr Opin Biotechnol 13:228–233. https://doi.org/10.1016/S0958-1669(02)00318-X
137. Verstraeten N, Braeken K, Debkumari B et al (2008) Living on a surface: swarming and biofilm formation. Trends Microbiol 16:496–506. https://doi.org/10.1016/j.tim.2008.07.004
138. Zhang X, Bishop PL, Kupferle MJ (1998) Measurement of polysaccharides and proteins in biofilm extracellular polymers. Water Sci Technol 37:345–348. https://doi.org/10.1016/S0273-1223(98)00127-9
139. Sutherland IW (2001) Biofilm exopolysaccharides: a strong and sticky framework. Microbiology 147:3–9. https://doi.org/10.1099/00221287-147-1-3
140. Sutherland IW (2001) The biofilm matrix—an immobilized but dynamic microbial environment. Trends Microbiol 9:222–227. https://doi.org/10.1016/S0966-842X(01)02012-1
141. Flemming HC, Wingender J (2010) The biofilm matrix. Nat Rev Microbiol 8:623–633. https://doi.org/10.1038/nrmicro2415
142. Flemming H-C (1995) Sorption sites in biofilms. Water Sci Technol 32:27–33. https://doi.org/10.1016/0273-1223(96)00004-2
143. Flemming H-C (2009) Why microorganisms live in biofilms and the problem of biofouling. In: Flemming HC, Murthy PS, Venkatesan RCK (ed) Marine and industrial biofouling. Springer Berlin Heidelberg
144. Banerjee S, Joshi SR (2013) Insights into cave architecture and the role of bacterial biofilm. Proc Natl Acad Sci India Sect B - Biol Sci 83:277–290. https://doi.org/10.1007/s40011-012-0149-3
145. van Hullebusch ED, Zandvoort MH, Lens PNL (2003) Metal immobilisation by biofilms: mechanisms and analytical tools. Rev Environ Sci Biotechnol 2:9–33. https://doi.org/10.1023/B:RESB.0000022995.48330.55
146. Beveridge TJ, Makin SA, Kadurugamuwa JL, Li Z (1997) Interactions between biofilms and the environment. FEMS Microbiol Rev 20:291–303. https://doi.org/10.1016/S0168-6445(97)00012-0
147. Tsezos M (2007) Biological removal of ions: principles and applications. Adv Mater Res 20–21:589–596. https://doi.org/10.4028/www.scientific.net/amr.20-21.589
148. Ferris FG, Schultze S, Witten TC et al (1989) Metal interactions with microbial biofilms in acidic and neutral pH environments. Appl Environ Microbiol 55:1249–1257. https://doi.org/10.1128/aem.55.5.1249-1257.1989
149. Gadd GM (2001) Phytoremediation of toxic metals; using plants to clean up the environment. John Wiley & Sons, Ltd
150. McLean RJC, Fortin D, Brown DA (1996) Microbial metal-binding mechanisms and their relation to nuclear waste disposal. Can J Microbiol 42:392–400. https://doi.org/10.1139/m96-055
151. Yee N, Fein J (2001) Cd adsorption onto bacterial surfaces: a universal adsorption edge? Geochim Cosmochim Acta 65:2037–2042. https://doi.org/10.1016/S0016-7037(01)00587-7
152. Gadd GM (2010) Metals, minerals and microbes: Geomicrobiology and bioremediation. Microbiology 156:609–643. https://doi.org/10.1099/mic.0.037143-0
153. Gourdon R, Bhende S, Rus E, Sofer SS (1990) Comparison of cadmium biosorption by Gram-positive and Gram-negative bacteria from activated sludge. Biotechnol Lett 12:839–842. https://doi.org/10.1007/BF01022606
154. Schorer M, Eisele M (1997) Accumulation of inorganic and organic pollutants by biofilms in the aquatic environment. Water, Air Soil Pollut 99:651–659. https://doi.org/10.1023/A:1018384616442
155. Konhauser KO (1998) Diversity of bacterial iron mineralization. Earth-Sci Rev 43:91–121. https://doi.org/10.1016/S0012-8252(97)00036-6
156. Ferris FG, Beveridge TJ (1986) Physiochemical roles of soluble metal cations in the outer membrane of *Escherichia coli* K-12. Can J Microbiol 32:594–601. https://doi.org/10.1139/m86-110

157. Beveridge TJ (1978) The response of cell walls of Bacillus subtilis to metals and to electron-microscopic stains. Can J Microbiol 24:89–104. https://doi.org/10.1139/m78-018
158. Violante A, Zhu J, Pigna M et al (2013) Role of biomolecules in influencing transformation mechanisms of metals and metalloids in soil environments. Mol Environ Soil Sci. https://doi.org/10.1007/978-94-007-4177-5_7
159. Mann S (1983) Mineralization in biological systems. Inorganic elements in biochemistry. Springer, Berlin Heidelberg, Berlin, Heidelberg, pp 125–174
160. Gaillardet J, Viers J, Dupré B (2003) Trace elements in river waters. Treatise Geochem 5–9:225–272. https://doi.org/10.1016/B0-08-043751-6/05165-3
161. Inskeep WP, Macur RE, Harrison G et al (2004) Biomineralization of As(V)-hydrous ferric oxyhydroxide in microbial mats of an acid-sulfate-chloride geothermal spring, Yellowstone National Park. Geochim Cosmochim Acta 68:3141–3155. https://doi.org/10.1016/j.gca.2003.09.020
162. He K, Roud SC, Gilder SA et al (2018) Seasonal variability of magnetotactic bacteria in a freshwater pond. Geophys Res Lett 45:2294–2302. https://doi.org/10.1002/2018GL077213
163. Peng XT, Zhou HY, Yao HQ et al (2007) Microbe-related precipitation of iron and silica in the Edmond deep-sea hydrothermal vent field on the Central Indian Ridge. Chin Sci Bull 52:3233–3238. https://doi.org/10.1007/s11434-007-0523-3
164. Konhauser KO, Schultze-Lam S, Ferris FG et al (1994) Mineral precipitation by epilithic biofilms in the speed river, Ontario, Canada. Appl Environ Microbiol 60:549–553. https://doi.org/10.1128/aem.60.2.549-553.1994
165. Cosmidis J, Benzerara K, Morin G et al (2014) Biomineralization of iron-phosphates in the water column of Lake Pavin (Massif Central, France). Geochim Cosmochim Acta 126:78–96. https://doi.org/10.1016/j.gca.2013.10.037
166. Clarke WA, Konhauser KO, Thomas JC, Bottrell SH (1997) Ferric hydroxide and ferric hydroxysulfate precipitation by bacteria in an acid mine drainage lagoon. FEMS Microbiol Rev 20:351–361. https://doi.org/10.1016/S0168-6445(97)00017-X
167. Konhauser KO, Fisher QJ, Fyfe WS et al (1998) Authigenic mineralization and detrital clay binding by freshwater biofilms: the brahmani river, India. Geomicrobiol J 15:209–222. https://doi.org/10.1080/01490459809378077
168. Konhauser KO, Ferris FG (1996) Diversity of iron and silica precipitation by microbial mats in hydrothermal waters, Iceland: implications for Precambrian iron formations. Geology 24:323–326. https://doi.org/10.1130/0091-7613(1996)024%3c0323:DOIASP%3e2.3.CO;2
169. Benzerara K, Morin G, Yoon TH et al (2008) Nanoscale study of As biomineralization in an acid mine drainage system. Geochim Cosmochim Acta 72:3949–3963. https://doi.org/10.1016/j.gca.2008.05.046
170. Sanna R, De Giudici G, Scorciapino AM et al (2013) Investigation of the hydrozincite structure by infrared and solid-state NMR spectroscopy. Am Mineral 98:1219–1226. https://doi.org/10.2138/am.2013.4158
171. Medas D, Meneghini C, Podda F et al (2018) Structure of low-order hemimorphite produced in a Zn-rich environment by cyanobacterium *Leptolingbya frigida*. Am Mineral. https://doi.org/10.2138/am-2018-6128
172. Garcia-Guinea J, Garrido F, Lopez-Arce P et al (2016) Analyzing materials in the microscopes: From the Sorby thin sections up to the non-destructive large chambers. AIP Conf Proc 1742:20002. https://doi.org/10.1063/1.4953121
173. Kochian LV (2012) Rooting for more phosphorus. Nature 488:466–467. https://doi.org/10.1038/488466a
174. Gianinazzi-Pearson V (1996) Plant cell responses to arbuscular mycorrhizal fungi: getting to the roots of the symbiosis. Plant Cell 8:1871–1883. https://doi.org/10.1105/tpc.8.10.1871
175. Bonneville S, Smits MM, Brown A et al (2009) Plant-driven fungal weathering: early stages of mineral alteration at the nanometer scale. Geology 37:615–618. https://doi.org/10.1130/G25699A.1

176. Bonneville S, Morgan DJ, Schmalenberger A et al (2011) Tree-mycorrhiza symbiosis accelerate mineral weathering: evidences from nanometer-scale elemental fluxes at the hypha-mineral interface. Geochim Cosmochim Acta 75:6988–7005. https://doi.org/10.1016/j.gca.2011.08.041
177. Moulton KL, West J, Berner RA (2000) Solute flux and mineral mass balance approaches to the quantification of plant effects on silicate weathering. Am J Sci 300:539–570. https://doi.org/10.2475/ajs.300.7.539
178. Chorover J, Kretzschmar R, Garica-Pichel F, Sparks DL (2007) Soil biogeochemicial processes within the critical zone. Elements 3:321–326. https://doi.org/10.2113/gselements.3.5.321
179. Landeweert R, Hoffland E, Finlay RD et al (2001) Linking plants to rocks: ectomycorrhizal fungi mobilize nutrients from minerals. Trends Ecol Evol 16:248–254. https://doi.org/10.1016/S0169-5347(01)02122-X
180. Lambers H, Mougel C, Jaillard B, Hinsinger P (2009) Plant-microbe-soil interactions in the rhizosphere: an evolutionary perspective. Plant Soil 321:83–115. https://doi.org/10.1007/s11104-009-0042-x
181. Song Z, Wang H, Strong PJ et al (2012) Plant impact on the coupled terrestrial biogeochemical cycles of silicon and carbon: implications for biogeochemical carbon sequestration. Earth-Sci Rev 115:319–331. https://doi.org/10.1016/j.earscirev.2012.09.006
182. Conley DJ (2002) Terrestrial ecosystems and the global biogeochemical silica cycle. Global Biogeochem Cycles 16:68. https://doi.org/10.1029/2002GB001894
183. Tréguer P, Nelson DM, Van Bennekom AJ et al (1995) The silica balance in the world ocean: A reestimate. Science 268(80):375–379. https://doi.org/10.1126/science.268.5209.375
184. Alexandre A, Colin F, Meunier J-D (1994) Phytoliths as indicators of the biogeochemical turnover of silicon in equatorial rainforest. Comptes Rendus - Acad des Sci Ser II Sci la Terre des Planetes 319:453–458
185. Cary L, Alexandre A, Meunier J-D et al (2005) Contribution of phytoliths to the suspended load of biogenic silica in the Nyong basin rivers (Cameroon). Biogeochemistry 74:101–114. https://doi.org/10.1007/s10533-004-2945-1
186. Fraysse F, Cantais F, Pokrovsky OS et al (2006) Aqueous reactivity of phytoliths and plant litter: physico-chemical constraints on terrestrial biogeochemical cycle of silicon. J Geochemical Explor 88:202–205. https://doi.org/10.1016/j.gexplo.2005.08.039
187. Adrees M, Ali S, Rizwan M et al (2015) Mechanisms of silicon-mediated alleviation of heavy metal toxicity in plants: a review. Ecotoxicol Environ Saf 119:186–197. https://doi.org/10.1016/j.ecoenv.2015.05.011
188. Hinsinger P (2011) Biogeochemical, biophysical, and biological processes in the rhizosphere. In: Huang PM, Li Y, Summer ME (eds) Handbook of soil science resource of management and environmental impacts. CRC Press, Taylor & Francis, pp 1–30
189. Violante A, Caporale AG (2015) Biogeochemical processes at soil-root interface. J Soil Sci Plant Nutr 15:422–448. https://doi.org/10.4067/s0718-95162015005000038
190. Chen YT, Wang Y, Yeh KC (2017) Role of root exudates in metal acquisition and tolerance. Curr Opin Plant Biol 39:66–72. https://doi.org/10.1016/j.pbi.2017.06.004
191. Zhu Y, Duan G, Chen B et al (2014) Mineral weathering and element cycling in soil-microorganism-plant system. Sci China Earth Sci 57:888–896. https://doi.org/10.1007/s11430-014-4861-0
192. Antoniadis V, Levizou E, Shaheen SM et al (2017) Trace elements in the soil-plant interface: phytoavailability, translocation, and phytoremediation–a review. Earth-Science Rev 171:621–645. https://doi.org/10.1016/j.earscirev.2017.06.005
193. Viehweger K (2014) How plants cope with salinity. Bot Stud 55:1–8
194. Xu B, Yu S (2013) Root iron plaque formation and characteristics under N_2 flushing and its effects on translocation of Zn and Cd in paddy rice seedlings (*Oryza sativa*). Ann Bot 111:1189–1195. https://doi.org/10.1093/aob/mct072
195. Chang H, Buettner SW, Seaman JC et al (2014) Uranium immobilization in an iron-rich rhizosphere of a native wetland plant from the Savannah River site under reducing conditions. Environ Sci Technol 48:9270–9278. https://doi.org/10.1021/es5015136

196. Tripathi RD, Tripathi P, Dwivedi S et al (2014) Roles for root iron plaque in sequestration and uptake of heavy metals and metalloids in aquatic and wetland plants. Metallomics 6:1789–1800. https://doi.org/10.1039/c4mt00111g
197. Hansel CM, Fendorf S, Sutton S, Newville M (2001) Characterization of Fe plaque and associated metals on the roots of mine-waste impacted aquatic plants. Environ Sci Technol 35:3863–3868. https://doi.org/10.1021/es0105459
198. Medas D, De Giudici G, Casu MA et al (2015) Microscopic processes ruling the bioavailability of Zn to roots of *Euphorbia Pithyusa* L. Pioneer plant. Environ Sci Technol 49:1400–1408. https://doi.org/10.1021/es503842w
199. De Giudici G, Medas D, Meneghini C et al (2015) Microscopic biomineralization processes and Zn bioavailability: a synchrotron-based investigation of *Pistacia lentiscus* L. roots. Environ Sci Pollut Res 22:19352–19361. https://doi.org/10.1007/s11356-015-4808-9
200. Mani D, Kumar C (2014) Biotechnological advances in bioremediation of heavy metals contaminated ecosystems: an overview with special reference to phytoremediation. Int J Environ Sci Technol 11:843–872. https://doi.org/10.1007/s13762-013-0299-8
201. He H, Veneklaas EJ, Kuo J, Lambers H (2014) Physiological and ecological significance of biomineralization in plants. Trends Plant Sci 19:166–174. https://doi.org/10.1016/j.tplants.2013.11.002
202. Medas D, De Giudici G, Pusceddu C et al (2019) Impact of Zn excess on biomineralization processes in *Juncus acutus* grown in mine polluted sites. J Hazard Mater 370:98–107. https://doi.org/10.1016/j.jhazmat.2017.08.031
203. Boi ME, Medas D, Aquilanti G, et al (2020) Mineralogy and Zn chemical speciation in a soil-plant system from a metal-extreme environment: a study on *Helichrysum microphyllum* subsp. tyrrhenicum (Campo Pisano Mine, SW Sardinia, Italy). Minerals 10:259. https://doi.org/10.3390/min10030259
204. McNear DH, Peltier E, Everhart J et al (2005) Application of quantitative fluorescence and absorption-edge computed microtomography to image metal compartmentalization in *Alyssum murale*. Environ Sci Technol 39:2210–2218. https://doi.org/10.1021/es0492034
205. Sarret G, Harada E, Choi YE et al (2006) Trichomes of tobacco excrete zinc as zinc-substituted calcium carbonate and other zinc-containing compounds. Plant Physiol 141:1021–1034. https://doi.org/10.1104/pp.106.082743
206. Reimann C, Englmaier P, Fabian K, et al (2015) Biogeochemical plant–soil interaction: variable element composition in leaves of four plant species collected along a south–north transect at the southern tip of Norway. Sci Total Environ 506–507:480–495. https://doi.org/10.1016/j.scitotenv.2014.10.079
207. Lanson B, Marcus MA, Fakra S et al (2008) Formation of Zn Ca phyllomanganate nanoparticles in grass roots. Geochim Cosmochim Acta 72:2478–2490. https://doi.org/10.1016/j.gca.2008.02.022
208. Van Balen E, Van De Geijn SC, Desmet GM (1980) Autoradiographic evidence for the incorporation of cadmium into calcium oxalate crystals. Z Pflanzenphysiol 97:123–133. https://doi.org/10.1016/s0044-328x(80)80026-2
209. Mazen AMA, El Maghraby OMO (1997) Accumulation of cadmium, lead and strontium, and a role of calcium oxalate in water hyacinth tolerance. Biol Plant 40:411–417. https://doi.org/10.1023/A:1001174132428
210. de la Fuente V, Rufo L, Juarez BH et al (2016) Formation of biomineral iron oxides compounds in a Fe hyperaccumulator plant: *Imperata cylindrica* (L.) P. Beauv. J Struct Biol 193:23–32. https://doi.org/10.1016/j.jsb.2015.11.005
211. Rodríguez N, Menéndez N, Tornero J et al (2005) Internal iron biomineralization in *Imperata cylindrica*, a perennial grass: chemical composition, speciation and plant localization. New Phytol 165:781–789. https://doi.org/10.1111/j.1469-8137.2004.01264.x
212. Liang Y, Sun W, Zhu Y-G, Christie P (2007) Mechanisms of silicon-mediated alleviation of abiotic stresses in higher plants: a review. Environ Pollut 147:422–428. https://doi.org/10.1016/j.envpol.2006.06.008

213. Neumann D, Nieden UZ, Schwieger W et al (1997) Heavy metal tolerance of *minuartia verna*. J Plant Physiol 151:101–108. https://doi.org/10.1016/S0176-1617(97)80044-2
214. Neumann D, zur Nieden U (2001) Silicon and heavy metal tolerance of higher plants. Phytochemistry 56:685–692. https://doi.org/10.1016/s0031-9422(00)00472-6
215. Moravec B, Chorover J (2020) Critical zone biogeochemistry. Biogeochem Cycles 131–149. https://doi.org/10.1002/9781119413332.ch6
216. NRC (2001) Basic research opportunities in the Earch sciences. National Academies Press, Washington
217. Giardino JR, Houser C (2015) Introduction to the critical zone. Dev Earth Surf Process 19:1–13. https://doi.org/10.1016/B978-0-444-63369-9.00001-X
218. White T, Brantley S, Banwart S et al (2015) The role of critical zone observatories in critical zone science. Elsevier B.V.
219. Brantley SL, Goldhaber MB, Vala Ragnarsdottir K (2007) Crossing disciplines and scales to understand the critical zone. Elements 3:307–314. https://doi.org/10.2113/gselements.3.5.307
220. Brantley SL, Eissenstat DM, Marshall JA et al (2017) Reviews and syntheses: on the roles trees play in building and plumbing the critical zone. Biogeosciences 14:5115–5142. https://doi.org/10.5194/bg-14-5115-2017
221. Sparks DL (2005) Toxic metals in the environment: the role of surfaces. Elements 1:193–197
222. Anderson SP, Von BF, White AF (2007) Physical and chemical controls on the critical zone. Elements 3:315–320. https://doi.org/10.2113/gselements.3.5.315
223. Perdrial J, Thompson A, Chorover J (2015) Soil geochemistry in the critical zone: influence on atmosphere, surface- and groundwater composition. In: Giardino JR (eds) Houser CBT-D in ESP. Elsevier, pp 173–201
224. Manceau A, Tamura N, Celestre RS et al (2003) Molecular-scale speciation of Zn and Ni in soil ferromanganese nodules from loess soils of the Mississippi basin. Environ Sci Technol 37:75–80. https://doi.org/10.1021/es025748r
225. Coston JA, Fuller CC, Davis JA (1995) Pb^{2+} and Zn^{2+} adsorption by a natural aluminum and iron-beariring surface coating on an aquifer sand. 59:3535–3547. https://doi.org/10.1016/0016-7037(95)00231-N
226. Davranche M, Gélabert A, Benedetti MF (2020) Electron transfer drives metal cycling in the critical zone. Elements 16:185–190. https://doi.org/10.2138/gselements.16.3.185
227. Gadd GM (2010) Microbial role in global biogeochemical cycling of metals and metalloids at the interfaces in the earth's critical zone. Mol Environ Soil Sci Interfaces Earth's Crit Zo. https://doi.org/10.1007/978-3-642-05297-2_2
228. Gadd GM (2013) Molecular environmental soil science. Springer, Dordrecht
229. Boulton AJ, Findlay S, Marmonier P et al (1998) The functional significance of the hyporheic zone in streams and rivers. Annu Rev Ecol Syst 29:59–81. https://doi.org/10.1146/annurev.ecolsys.29.1.59
230. Hoagland B, Russo TA, Brantley SL (2017) Relationships in a headwater sandstone stream. Water Resour Res Res 53:4643–4667. https://doi.org/10.1002/2016WR019717.Received
231. Mcintosh J, Schaumberg C, Perdrial J et al (2017) Geochemical evolution of the Critical Zone across variable time scales informs concentration-discharge relationships: Jemez River Basin Critical Zone Observatory. Water Resour Res 53:4169–4196. https://doi.org/10.1002/2016WR019712
232. Wondzell SM (2011) This file was created by scanning the printed publication. Text errors identified by the software have been corrected: however some errors may remain. The role of the hyporheic zone across stream networks t. Hydrol Process 25:3525–3532
233. Watling HR (2006) The bioleaching of sulphide minerals with emphasis on copper sulphides—a review. Hydrometallurgy 84:81–108. https://doi.org/10.1016/J.HYDROMET.2006.05.001
234. Brar KK, Magdouli S, Etteieb S, et al (2021) Integrated bioleaching-electrometallurgy for copper recovery—a critical review. J Clean Prod 291:125257. https://doi.org/10.1016/j.jclepro.2020.125257

235. Mishra D, Kim D-J, Ahn J-G, Rhee Y-H (2005) Bioleaching: a microbial process of metal recovery; A review. Met Mater Int 11:249–256. https://doi.org/10.1007/BF03027450
236. Cecchi G, Marescotti P, Di Piazza S, Zotti M (2017) Native fungi as metal remediators: silver myco-accumulation from metal contaminated waste-rock dumps (Libiola Mine, Italy). J Environ Sci Heal Part B 52:191–195. https://doi.org/10.1080/03601234.2017.1261549
237. Rickard D (2012) Sulfidic sediments and sedimentary rocks. Elsevier
238. Ohmoto H, Lasaga AC (1982) Kinetics of reactions between aqueous sulfates and sulfides in hydrothermal systems. Geochim Cosmochim Acta 46:1727–1745. https://doi.org/10.1016/0016-7037(82)90113-2
239. Sato M (1992) Persistency-field Eh-pH diagrams for sulfides and their application to supergene oxidation and enrichment of sulfide ore bodies. Geochim Cosmochim Acta 56:3133–3156. https://doi.org/10.1016/0016-7037(92)90294-S
240. Wilkin RT, Barnes HL (1997) Formation processes of framboidal pyrite. Geochim Cosmochim Acta 61:323–339. https://doi.org/10.1016/S0016-7037(96)00320-1
241. Wilkin RT, Barnes HL, Brantley SL (1996) The size distribution of framboidal pyrite in modern sediments: an indicator of redox conditions. Geochim Cosmochim Acta 60:3897–3912. https://doi.org/10.1016/0016-7037(96)00209-8
242. Labrenz M, Druschel GK, Thomsen-Ebert T et al (2000) Formation of sphalerite (ZnS) deposits in natural biofilms of sulfate-reducing bacteria. Science 290(80):1744–1747. https://doi.org/10.1126/science.290.5497.1744
243. Zhuang W-Q, Fitts JP, Ajo-Franklin CM et al (2015) Recovery of critical metals using biometallurgy. Curr Opin Biotechnol 33:327–335. https://doi.org/10.1016/j.copbio.2015.03.019
244. Staicu LC, Wojtowicz PJ, Pósfai M, et al (2020) PbS biomineralization using cysteine: *Bacillus cereus* and the sulfur rush. FEMS Microbiol Ecol 96:fiaa151. https://doi.org/10.1093/femsec/fiaa151
245. Paganin P, Alisi C, Dore E et al (2021) Microbial diversity of bacteria involved in biomineralization processes in mine-impacted freshwaters. Front Microbiol 12:778199. https://doi.org/10.3389/fmicb.2021.778199
246. De Giudici G, Wanty RB, Podda F et al (2014) Quantifying biomineralization of zinc in the Rio Naracauli (Sardinia, Italy), using a tracer injection and synoptic sampling. Chem Geol 384:110–119. https://doi.org/10.1016/j.chemgeo.2014.07.002
247. De Giudici G, Pusceddu C, Medas D et al (2017) The role of natural biogeochemical barriers in limiting metal loading to a stream affected by mine drainage. Appl Geochemistry 76:124–135. https://doi.org/10.1016/j.apgeochem.2016.11.020